
Myriam Jessica Visram

0731597

Lipid Metabolism during the Cell Cycle in Yeast

Saccharomyces cerevisiae

Master Thesis

To obtain the academic degree of

„MSc Master of Science“

in the subject “Biochemistry and Molecular Biomedical Science”

at the Technical University of Graz

Supervisors:

Mag. Dr. Gerald N. Rechberger

Univ.-Prof. DI Dr. Sepp D. Kohlwein

Institute of Molecular Biosciences

Karl-Franzens University Graz

2011/2012

STATUTORY DECLARATION

I declare that I have authored this thesis independently, that I have not used other than the declared sources / resources, and that I have explicitly marked all material which has been quoted either literally or by content from the used sources.

.....
Date

.....
Signature

EIDESSTATTLICHE ERKLÄRUNG

Ich erkläre an Eides statt, dass ich die vorliegende Arbeit selbstständig verfasst, andere als die angegebenen Quellen/Hilfsmittel nicht benutzt, und die den benutzten Quellen wörtlich und inhaltlich entnommene Stellen als solche kenntlich gemacht habe.

Graz, am

.....

(Unterschrift)

Special Thanks To...

... Univ.-Prof. DI Dr. Sepp D. Kohlwein for giving me the opportunity to do this work in his lab, and for always being such a motivating and encouraging teacher.

... Mag. Dr. Gerald N. Rechberger for his supervision, help and advice at work and outside. He made my time in this group unforgettable in so many ways.

... MSc Neha Chauhan, who in addition to being an exceptionally gifted teacher, became a very close friend. Her unlimited patience and guidance made my work better. Her heart and her wacky sense of humor made my work fun!

... all my colleagues in the Kohlwein group. You made me feel very much at home! Thank you for your unlimited supply of word-jokes and for making me laugh until tears run down my face!

...Tim, for his help and friendship in all situations!

...my friends Katy and Rosa, who redefine the words loyalty, support and unconditional friendship.

... Daniel, who is the brother I never had and an anchor to the family!

... my sister Zehra, my confidante, who in addition to being my own personal scientific advisor, always has an open ear, a glass of wine and a good piece of advice. Without her support, none of this would have been possible.

... my father Mo, who unfortunately is not here to celebrate with me. He is sorely missed every day! His sharp mind, wild sense of humor and unique ability to enjoy life in all its aspects made him a true citizen of the world!

..and last but not least..

I would like extend my deepest gratitude to my mother Jeanne. Without her unending support and encouragement, I would not have been able to finish this degree. Her courage and strength will always be an inspiration to me.

Index

1. Abstract.....	8
1.1. Abstract.....	8
1.2. Kurzfassung	9
2. Table of abbreviations	10
3. Introduction.....	12
3.1. Lipid metabolism	12
3.2. Lipid link to cell cycle	15
3.2.1. Cell cycle & growth phases	15
3.2.2. Cyclin dependent kinases, lipolysis and their link to the cell cycle.....	17
4. Aim & Experimental setup	19
4.1. Aim	19
4.2. Experimental setup.....	19
5. Results & Discussion	21
5.1. Synchronisation: gradient centrifugation with RediGrad®	21
5.2. Growth	22
5.3. FACS: Fluorescence activated cell sorting	23
5.4. Cell cycle results for WT and the <i>swel</i> , <i>tgl3tgl4</i> and <i>tgl3tgl4swel</i> mutants	24
5.4.1. Triacylglycerol (TAG).....	24
5.4.2. Diacylglycerol (DAG)	32
5.4.3. Phosphatidic acid (PA)	36
5.4.4. Phosphatidylinositol (PI)	40
5.4.5. Phosphatidylserine (PS).....	42
5.4.6. Phosphatidylethanolamine (PE).....	44
5.4.7. Phosphatidylcholine (PC)	46
5.5. Growth phase results for WT and the <i>swel</i> , <i>tgl3tgl4</i> , <i>tgl3tgl4swel</i> mutants....	50
5.5.1. Triacylglycerol (TAG).....	50
5.5.2. Diacylglycerol (DAG)	54
5.5.3. Phosphatidic acid (PA)	55
5.5.4. Phosphatidylinositol (PI)	56

5.5.5.	Phosphatidylserine (PS)	57
5.5.6.	Phosphatidylethanolamine (PE)	59
5.5.7.	Phosphatidylcholine (PC)	60
5.6.	Further discussion	61
6.	Conclusions	63
7.	Materials & Methods	66
7.1.	Strains and Media	66
7.2.	Synchronisation	67
7.3.	Growth	67
7.4.	Lipid extraction and UPLC-qTOF-MS measurements	67
7.5.	FACS analysis (fluorescence activated cell sorting)	68
8.	Annexe	69
8.1.	SOP	69
8.1.1.	RediGrad Centrifugation	69
8.1.2.	FACS	70
8.1.3.	LE	70
9.	References	72

1. Abstract

1.1. Abstract

During cell division many components of the cell such as DNA or membranes are synthesised to provide the emerging daughter cell with the necessary equipment to live independently. Previous work done in our group demonstrated a link between lipid homeostasis (lipolysis) and cell cycle progression. It was demonstrated that the cyclin dependent kinase Cdc28p, the major regulator of the cell cycle, governs the activity of Tgl4p, a major triacylglycerol lipase in *Saccharomyces cerevisiae*. These findings raised the question as to what lipid species originating from TAG degradation are required for cell cycle progression and which “check-point” monitors the availability of these compounds. One potential candidate is Swe1p. At the G2/M phase of the cell cycle it phosphorylates and inhibits Cdc28p and thereby stalling the cell cycle until certain requirements such as cell size are met. It was also observed that deletion of *SWE1* recovers a G1/S delay in the cell cycle in the *tgl3tgl4* mutant.

By analysing lipid profiles obtained by UPLC-qTOF-MS of the strains described previously we found that Swe1p has a direct effect on lipid metabolism. It was observed that in all strains the main TAG species that are degraded during the cell cycle are unsaturated, and this also reflects on the profiles obtained for the other lipid classes. It was also seen that the *tgl3tgl4* and *tgl3tgl4swe1* lipase mutants show residual lipolytic activity during the cell cycle suggesting the presence of another lipase. These lipid profiles also indicate that Swe1p might show acyltransferase activity, and that the lipase mutants have a compensatory mechanism to counteract the lack of lipolysis.

1.2. Kurzfassung

Während des Zellzyklus werden viele Komponenten der Zelle, wie zum Beispiel DNA oder Membranen, repliziert oder synthetisiert damit die Tochterzelle unabhängig funktionieren kann. Unsere Gruppe hat vor einiger Zeit den Zusammenhang zwischen Lipolyse und dem zeitlichen Ablauf des Zellzyklus demonstriert. Die Zyklin-abhängige Kinase Cdc28p reguliert den Zellzyklus und hat einen stimulierenden Effekt auf Tgl4p, eine Triglyzeridlipase in *Saccharomyces cerevisiae*. Diese Ergebnisse haben verschiedene Fragen aufgeworfen. Welche Abbau-Produkte von TAG spielen eine Rolle im zeitlichen Verlauf des Zellzyklus und welche “check-points” kontrollieren diese Substanzen? Ein guter Kandidat fuer das Letztere ist Swe1p. Am G2/M Uebergang im Zellzyklus phosphoryliert diese Kinase Cdc28p, was zu einer Verzögerung des Zellzyklus führt bis verschiedene Kriterien wie zum Beispiel Zellgrösse erreicht sind.

Eine Analyse der Lipidprofile von verschiedenen Hefestämmen, die durch UPLC-qTOF-MS generiert wurden, hat ergeben dass Swe1p einen direkten Effekt auf den Lipidmetabolismus der Zelle hat. Es wurde beobachtet dass in allen Stämmen eher ungesättigte TAG Spezies im Zellzyklus abgebaut werden und dass sich dieser Abbau in den Profilen anderer Lipid Klassen widerspiegelt. Es wurde auch beobachtet dass die Lipase Mutanten *tgl3tgl4* und *tgl3tgl4swe1* eine lipolytische Aktivität aufweisen, was auf die Präsenz einer weiteren Lipase deutet. Diese Lipidprofile haben auch gezeigt dass Swe1p möglicherweise Azyltransferaseaktivität aufweist und dass die Lipase Mutanten einen Ausgleichsmechanismus besitzen, der die fehlende Lipolyse ausbalanciert.

2. Table of abbreviations

ATGL	Adipose triglyceride lipase
CDK	Cyclin dependent kinase
CDP-DAG	Cytidine diphosphate-diacylglycerol
DAG	Diacylglycerol
DNA	Deoxyribonucleic acid
FA	Fatty acids
FACS	Fluorescence activated cell sorting
G0 phase	Gap 0 phase
G1 phase	Gap 1 phase
G2-phase	Gap 2 phase
IST	Internal standard
LE	Lipid extraction
MAG	Monoacylglycerol
M-phase	Mitosis phase
ONC	Over night culture
PA	Phosphatidic acid
PC	Phosphatidylcholine
PE	Phosphatidylethanolamine
PI	Phosphatidylinositol
PIP	Phosphatidylinositol phosphate
PL	Phospholipid
PLC	Phospholipase C
PS	Phosphatidylserine
qTOF-MS	Quadrupol time of flight mass spectrometry
RNA	Ribonucleic acid
SL	Sphingolipid
S-phase	DNA synthesis phase (cell cycle)
TAG	Triacylglycerol

Tgl3p,4p,5p	Triacylglycerol lipase 3,4,5
UPLC	Ultra performance liquid chromatography
VLCFA	Very long chain fatty acid
WT	Wild type
YNB	Yeast nitrogen base
YPD	Yeast extract peptone dextrose
7DC	7 day culture

3. Introduction

3.1. Lipid metabolism

The last decade has shown an alarming increase in life-style related pathologies such as obesity, diabetes and cancer. Lipids play an important role in these afflictions and research on lipids in general helps elucidate certain aspects of these diseases. Lipids are important molecules in all cells and they play various roles in their morphology, regulation and survival. The yeast *Saccharomyces cerevisiae* offers itself as an attractive model organism to study the role of lipids in eukaryotic cells. It is easy to handle, and discoveries made in yeast often give insights into the biochemistry and physiology of more complex organisms, as many processes are conserved between yeast and higher eukaryotes. Lipids are involved in many aspects of a cells life. They are part of the membranes; act as storage molecules or even play a role in signalling. **Figure 3.1** shows a simplified view of lipid metabolism with species and connections relevant to this thesis. Lipids can be classified in two major groups, namely neutral lipids and polar lipids. Neutral lipids encompass species such as triacylglycerol (TAG) or diacylglycerol (DAG), amongst others. TAGs are molecules that act as energy storage components in the cell. They are buffer systems to store fatty acids (FA), as high concentrations of free FA are toxic to cells. A typical structure of a TAG would involve a glycerol molecule esterified with three fatty acyl chains, which can vary in their length and degree of unsaturation. TAG metabolism needs to be tightly controlled, as TAGs need to be synthesised or degraded quickly and efficiently as a reaction to different environmental cues. TAG degradation occurs through the activity of TAG lipases. The main lipases in yeast are Tgl3p, Tgl4p and Tgl5p, and their activity results in the formation of DAG and monoacylglycerol (MAG). Tgl3p and Tgl4p were identified as the major lipolytic enzymes, with Tgl3p also showing activity as DAG lipase (Kurat et al., 2006; Rajakumari et al., 2008). Tgl4p was also identified as the functional ortholog of mammalian adipose triglyceride lipase ATGL, underlining the fact that many biochemical processes are conserved between yeast and higher eukaryotic organisms (Kurat et al., 2006).

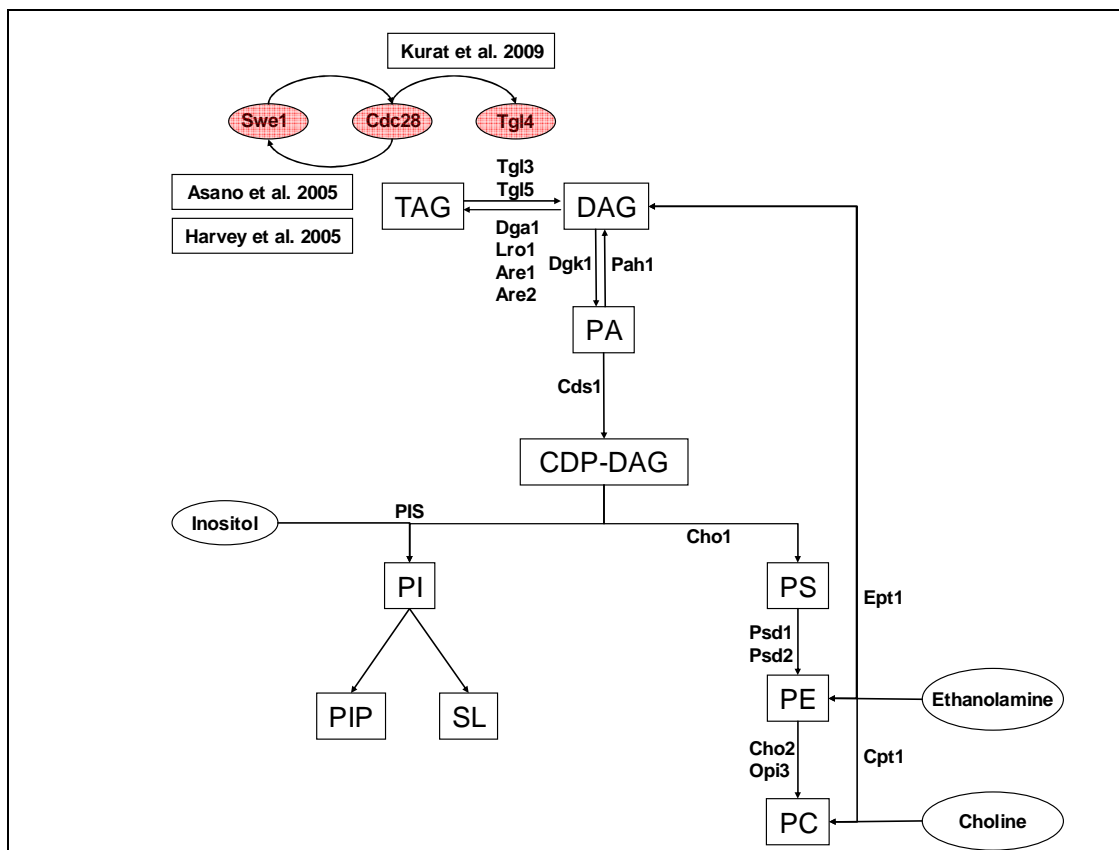


Figure 3.1: Overview Lipid Synthesis with link to the work of Asano et al. (2005), Harvey et al. (2005) and Kurat et al. (2009).

DAGs are formed from TAGs, by cleaving a single fatty acyl ester bond. However TAG degradation is not the only source of DAGs. They can be produced by many different other reactions, such as PL degradation by phospholipase C (PLC) or as a by-product in sphingolipid synthesis. Furthermore, DAG can also be formed by “*de novo* synthesis”. DAG levels are strictly regulated, as in addition to being an important intermediate, this class of lipids is also bioactive and plays a role in certain signalling pathways (Bielawska et al., 2001). **Figure 3.2** underlines the importance of a tight regulation of lipid metabolism. Although it shows the effect of DAG signalling in mammalian cells, it still demonstrates how DAG is involved in many biological processes, emphasizing once more the importance of a tight regulation.

Phosphatidic acid (PA) is at the cross-roads of lipid metabolism as it can be used to produce neutral and polar lipids, such as TAGs or phospholipids (PL) (C.f. **Figure 3.1**). Also the “*de novo*

synthesis” pathway will produce PA as a precursor to other lipids. Additionally to this PA is also bioactive and plays an important role in regulating lipid metabolism itself (Young et al., 2010).

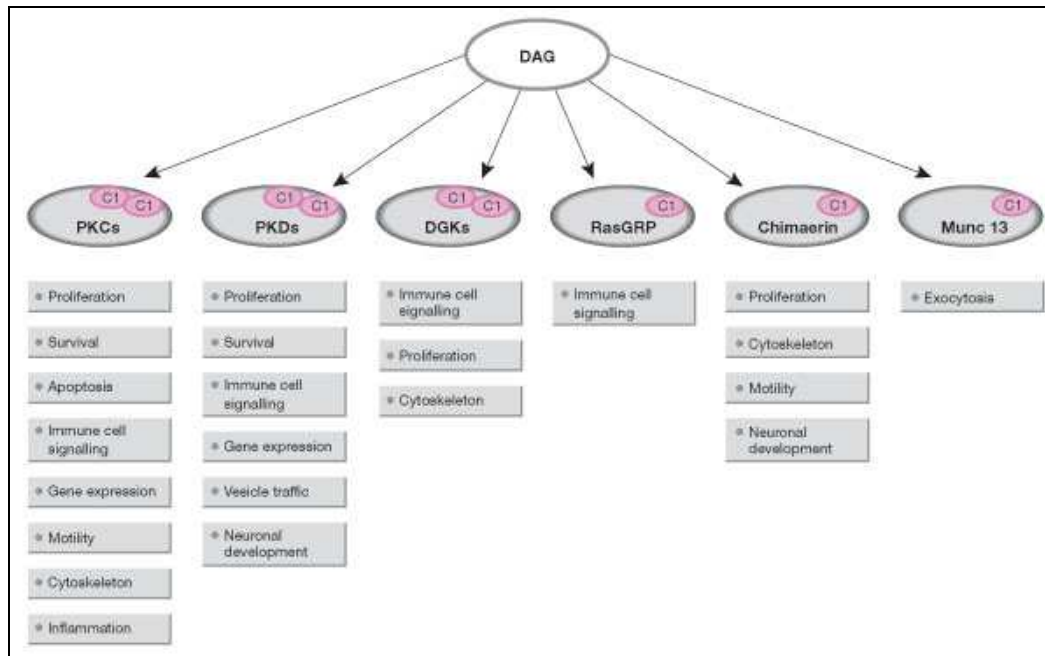


Figure 3.2: DAG signalling in mammalian cells (Toker; *EMBO reports* (2005) 6, 310 – 314).

The most notable polar lipids are the class of phospholipids (PL) such as phosphatidylcholine (PC), phosphatidylethanolamine (PE), phosphatidylserine (PS) and phosphatidylinositol (PI). These PLs are the major components of biological membranes, with PC and PE constituting the major building blocks for membranes. A typical structure of a PL describes a hydrophilic glycerol-3-phosphate head-group and a hydrophobic tail, made of two fatty acyl chains that can differ in length (mostly C16 or C18) or in their degree of unsaturation (0 or 1 double bond). The structure of the head groups differs for different PL species.

Figure 3.3 shows the flow of fatty acids in the general lipid metabolic pathway. Fatty acids are very versatile molecules and are used for many purposes. Lipids can be degraded and FAs used for energy production by β -oxidation in the peroxisomes. TAGs can be degraded and used to produce PL. The released FA's can be used for various purposes such as protein modification or remodelling of different lipid species.

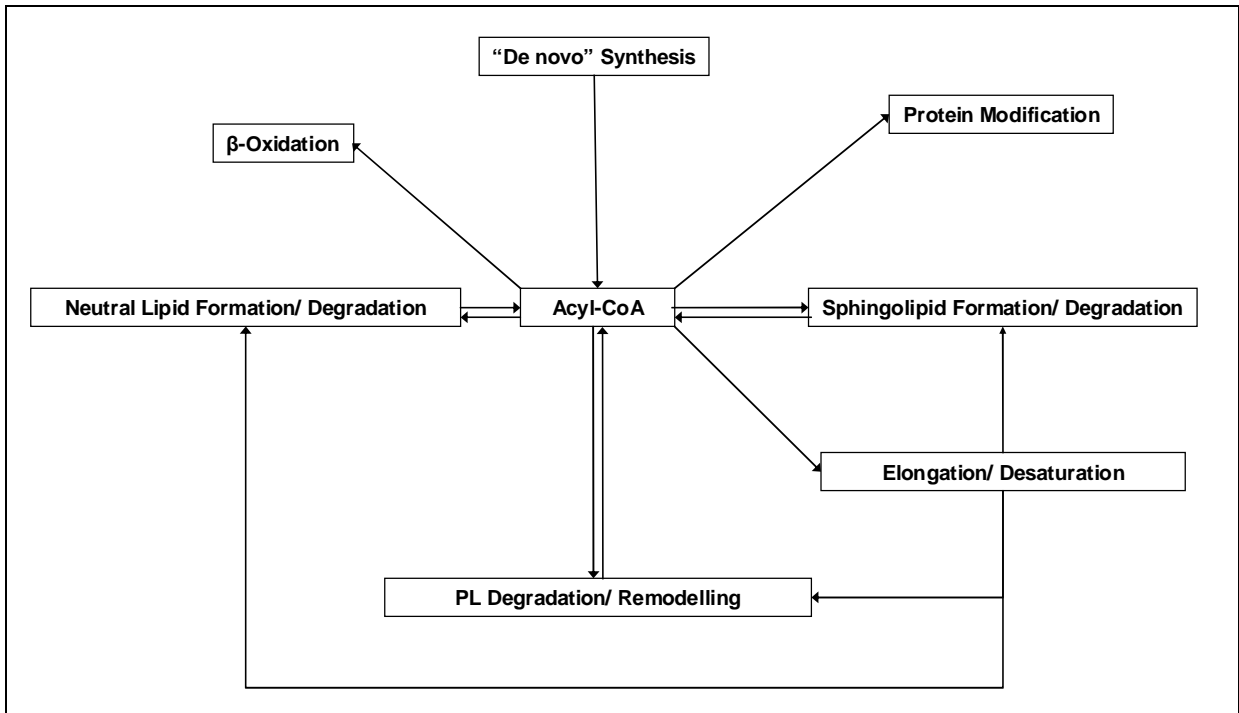


Figure 3.3: Fate of Acyl-CoAs (activated fatty acids) in the lipid metabolic pathway.

3.2. Lipid link to cell cycle

3.2.1. Cell cycle & growth phases

Cells grow and divide and for this they need to replicate their DNA and synthesise many essential components such as membranes. Defects in this process can lead to pathologies such as cancer and research on cell cycle can give very important insights to these diseases. The cell cycle is described as a series of events that lead to cell division and the production of a daughter cell, which contains chromosomes identical to those of the mother cell (Lodish et al., 2007).

The cell cycle can be divided in 4 phases, namely G1, S, G2 and M. **Figure 3.4** illustrates these 4 phases. During the G1 phase (Gap 1) cells grow in size and prepare for the S phase (synthesis phase) by synthesising proteins and machinery necessary to enter the next step. During the S-phase, the DNA set of the cell is replicated in preparation of division, as the daughter cell requires the complete replicated genome of the mother cell. The G2 (Gap 2) phase is an intermediate phase where cells prepare to enter mitosis or M-phase. During the M-phase the doubled DNA content

and the cellular content such as organelles are divided between the mother cell and the emerging daughter cell. Cytokinesis occurs at the end of the M-phase, producing a daughter cell from a mother cell. These cells then re-enter the cell cycle. (Lodish et al., 2007).

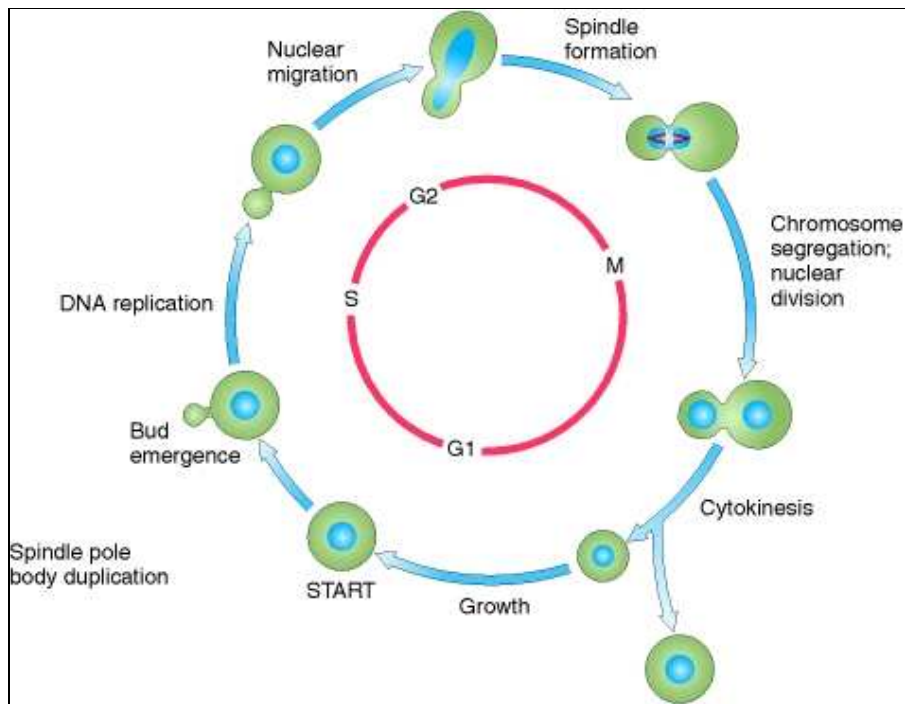


Figure 3.4: Illustration of the cell cycle in *S. cerevisiae* (Griffiths et al., 1999).

During this cell cycle, there are at least three check-points that allow the cell to recognize if all is running smoothly and if so, to transition into the next phase of the cell cycle. The START check-point in the G1 phase includes factors such as size, nutrient availability and genetic integrity. If some of the criteria are not met (e.g. availability of nutrients), the cells delay the cell cycle or alternatively exit the G1 phase, and enter quiescence, a state described subsequently as G0 (Lodish et al., 2007). The G0 phase, or stationary phase, is a coping mechanism used by cells, to ensure viability during times of nutrient limitation.

When cells are grown in culture, prior to entry into quiescence, several phases of growth can be distinguished. After stationary cells are transferred into a new nutrient-rich environment, they enter the lag-phase where they are biochemically active but have not started dividing yet. Cells adapt to their new environment (nutrient-rich), exit the stationary phase and prepare for re-entry into the

cell division cycle. When the cells start dividing again, they enter the log- or exponential phase. They will continue dividing until some nutrient is exhausted or some metabolite starts becoming toxic (Singh et al., 2006). When essential nutrients such as glucose are depleted, cells will enter the stationary phase again as a result of carbon starvation (Werner-Washburne M. et al., 1993).

TAG metabolism shows very notable differences during these different phases of growth. During the stationary phase, lipases are active and degrade TAGs slowly to provide FAs as an energy source. During the exit of the G0 phase, TAGs are degraded for different reasons. Their degradation products presumably provide precursors for PL synthesis, which allows a rapid initiation of growth. This TAG degradation is mainly performed by Tgl3p and Tgl4p. These enzymes work in parallel and independent of each other. It has been suggested that the activity of these lipases differs in different phases of growth; Tgl4p being the majorly active lipase during the lag-phase, and Tgl3p during the log-phase (Kurat et al., 2009; B. Weberhofer, Diploma Thesis 2010).

3.2.2. Cyclin dependent kinases, lipolysis and their link to the cell cycle

Cyclin dependent kinases (CDK) are heterodimer protein kinases that regulate the progression of a cell through its division cycle. CDKs are the catalytic subunits of a larger complex formed with cyclins, the regulatory subunits of the heterodimer. In yeast the concentrations and types of cyclins vary greatly over time and are dependent on the cell cycle phase the cells are in. The activity of cyclin associated CDK is highly regulated. The substrate specificity of each cyclin-CDK heterodimer is defined by the associated cyclin. Each CDK can associate with a number of different cyclins, which in turn determines the CDK's target proteins and, thus, activity. Cyclins Cln1p, Cln2p and Cln3p are the essential cyclins necessary to guide the cells from G1 to S-phase. The S-phase requires cyclins such as Clb5p and Clb6p. B-type cyclins such as Clb1p, Clb2p, Clb3p and Clb4p help the cells progression into the M-phase (Lodish et al., 2007; Wittenberg et al., 1990; Richardson et al., 1992).

Cdk1/Cdc28p is one of two cyclin dependent kinases in yeast and is of particular interest in this work. It has been shown that Cdc28p phosphorylates Tgl4p, a major TAG lipase in yeast. This phosphorylation activates Tgl4p, leading to a strongly increased TAG degradation. This TAG degradation presumably provides precursors for PL synthesis which are needed for membrane production during rapid initiation of growth (Kurat et al., 2009; Zanghellini et al., 2008).

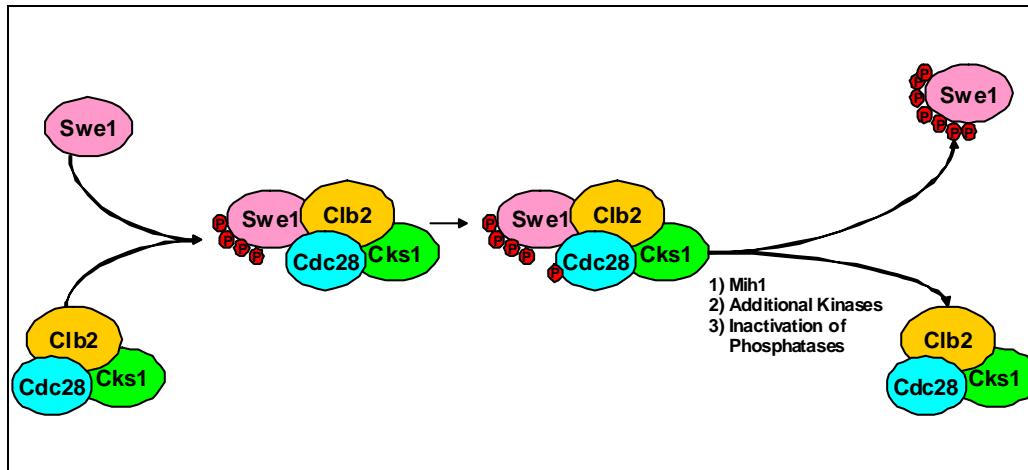


Figure 3.5: Interactions between Swe1p and Clb2-Cdc28 according to Harvey et al. (2005).

Swe1p is a protein kinase that acts as a morphogenesis checkpoint and regulates the cell's progression into mitosis (Lew et al. 2003). Check-points control key processes that are necessary for cell division, and if these requirements are not met, cell cycle check-points delay the cell cycle. Swe1p has such a check point function, and it delays the cell cycle at the G2/M transition in response to improper bud-formation by negatively regulating mitotic Clb2p cyclin associated Cdc28p (Sia et al., 1998). **Figure 3.5** shows the interactions between Swe1p and Cdc28p. Swe1p binds to Clb2-Cdc28p and gets phosphorylated by Cdc28p. This stabilises Swe1p and activates Swe1p tyrosine kinase activity. Swe1p then in return phosphorylates Cdc28p at a tyrosine (Y19) residue and inactivates the latter, leading to a delayed entry into mitosis. When the morphogenesis checkpoint requirements (such as cell size or actin organisation) are met, Mih1p phosphatase dephosphorylates Clb2-Cdc28p, reactivating it and leading the cell into mitosis. Swe1p is hyperphosphorylated and subsequently degraded. It has been suggested that Cdc28p plays a role in this hyperphosphorylation, as do the sites where this phosphorylation takes place (Sia et al., 1998; Harvey et al., 2005; Hu et al., 2008).

Kurat et al. (2009) proved the link between Cdc28p and Tgl4p during G1/S. Asano et al. (2005) and Harvey et al. (2005) demonstrated the link between Swe1p and Cdc28p during G2/M. This previous work does not directly link Swe1p to lipolysis, as the two effects described earlier take place at two different times during the cell cycle. Cdc28p and Tgl4p interaction occurs in the early phases of the cell cycle (Kurat et al., 2009), whereas the interaction between Cdc28p and Swe1p occurs in the late G2 phase (Harvey et al., 2005). Kurat et al. (2009) demonstrated a delay in the cell cycle of the *tgl3tgl4* deletion strain. Unpublished work by N. Chauhan shows that additional deletion of *SWE1* in this lipase deletion strains recovers this delay, suggesting an effect of Swe1p at the earlier stages of the cell cycle.

4. Aim & Experimental setup

4.1. Aim

The aim of this thesis was to identify a lipid-dependent checkpoint and to establish which TAG derived lipid species are critical to cell cycle progression and/or delay by observing lipid profiles of synchronised cells obtained from various deletion strains. This work should give an insight as to the effect of Swe1p on lipid metabolism and how the absence of this kinase manages to rescue a G1/S cell cycle delay caused by a lack of lipolysis.

4.2. Experimental setup

The experimental setup used was specially designed to address the aims of this thesis. Some aspects were already established methods and some were redefined for the purpose of these experiments. All results shown in the following section were obtained by experiments that followed the work flow described in **Figure 4.1** First the strains were cultured for two days on YPD plates and kept at 4°C until further use. An over-night culture (ONC) of the selected strain was made in YPD. Following this, a 7 day culture (7DC) was inoculated in YPD. After these 7 days, the quiescent cells in the G0 phase were separated from the non-quiescent and dead cells by

RediGrad® centrifugation (Allen et al., 2006). A cell count was performed using the CASY® Cell Counter and typically 5×10^8 cells were inoculated into fresh YNB media. The cells were counted and harvested at 30 minute intervals up to 240 minutes. In addition the cells were cultivated up to 72 hours and samples taken at 9h, 24h and 72h to assess lipid alterations during growth. The harvested cells were frozen in liquid nitrogen and stored at -80°C until lipid extraction was performed. An internal standard mix (IST) was added before each lipid extraction to aid in the later evaluation. Lipid extraction was performed according to the Standard Lab Operating Procedure (modified after Folch et al. (1957)). The lipid extracts were then analyzed by UPLC-ESI-qTOF-MS and the chromatograms and mass spectra obtained were evaluated using Waters® MassLynx™ and Lipid Data Analyzer Software (Hartler et al., 2010). For details on the standard operating procedures, materials and methods used please refer to section 7 and 8 of this thesis.

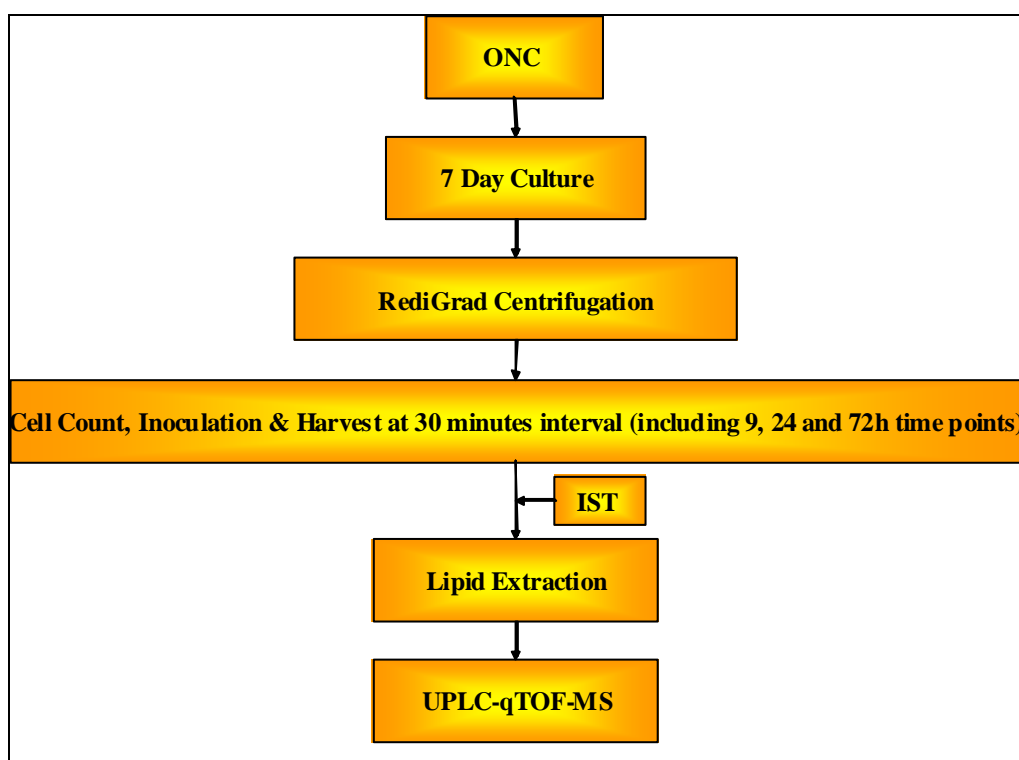


Figure 4.1: General work flow.

5. Results & Discussion

5.1. Synchronisation: gradient centrifugation with RediGrad®

A synchronised population of cells is in the same phase of the cell cycle. Various synchronisation techniques exist and all have their positive and negative sides. RediGrad® centrifugation was used in these experiments as they were designed to reproduce results observed by Kurat et al. (2009). For a detailed review on different synchronisation techniques please refer to C. Taus: Diploma Thesis 2010. The main attribute of this technique was that there was no chemical influence on the cells, as observed for example with an α -factor arrest. The mating pheromone α -factor arrests the cells in the G1 phase of the cell cycle, and prepares them for mating. This influences their biochemistry and might alter the outcome of the experiment. One drawback of gradient centrifugation is that the cells might not be as precisely synchronised as when α -factor is used. The general consensus states that cells enter quiescence when they are in the G1 phase, and they are in a situation of nutrient/carbon depletion. It has been shown, however, that cells cultured in a similar way to the culturing conditions described for these experiments, show a minor fraction of cells that enter quiescence at different stages of the cell cycle (Laporte et al., 2011). Laporte et al. (2011) describe the population as being composed of $90\pm 5\%$ unbudded cells (G1) and $10\pm 5\%$ of budded cells (S/G2). This means the cells separated by RediGrad® centrifugation may contain a small fraction of cells that will not re-enter the cell cycle at the G1 phase.

Previous FACS experiments (not shown here, N. Chauhan) suggested that at 0min there was a small part of the cell population that had a double set of chromosomes ($2n$). It was thought that this was due to cells sticking together. However the observations of Laporte et al. (2011) suggest that a small percentage of the cells possess 2 sets of chromosomes, however this percentage is insignificant. A viable alternative to the gradient centrifugation technique would be elutriation, where cells are separated according to their size (c.f.: C. Taus, Diploma Thesis 2010). There would be no chemical interaction with the cells, and a more precisely synchronised population could be obtained. Unfortunately this technique was not available in our lab.

5.2. Growth

During the experiments, approximately $5 \cdot 10^8$ cells were inoculated into fresh YNB media after synchronisation. During the harvest at 30min intervals, each culture was recounted to correct for pipetting errors. These measurements also provided the average size of the cells in culture and allowed to assess the change in size over time. **Figure 5.1** shows the development of cell volume over time for the 4 analysed strains. When considering the cell size and the FACS analysis (not depicted here), it could be seen that WT, *swe1* and *tgl3tgl4swe1* mutant populations started dividing between 150 and 180min, whereas the *tgl3tgl4* mutant only started dividing between 180 and 210min. This delay is not as obvious when only considering cell volume. The average volume seems to peak at 180min for all strains before it decreases again. Even if a fraction of the cells started dividing earlier, the majority of the population was still growing in size. Only when the majority of the cells have divided, will this reflect on the average volume. The “non-chemical” approach to synchronisation also has its draw-backs. The cells separated by gradient centrifugation are stationary and some cells might need longer to start dividing than others. It will therefore be assumed that the cells are synchronised only until 150-180min.

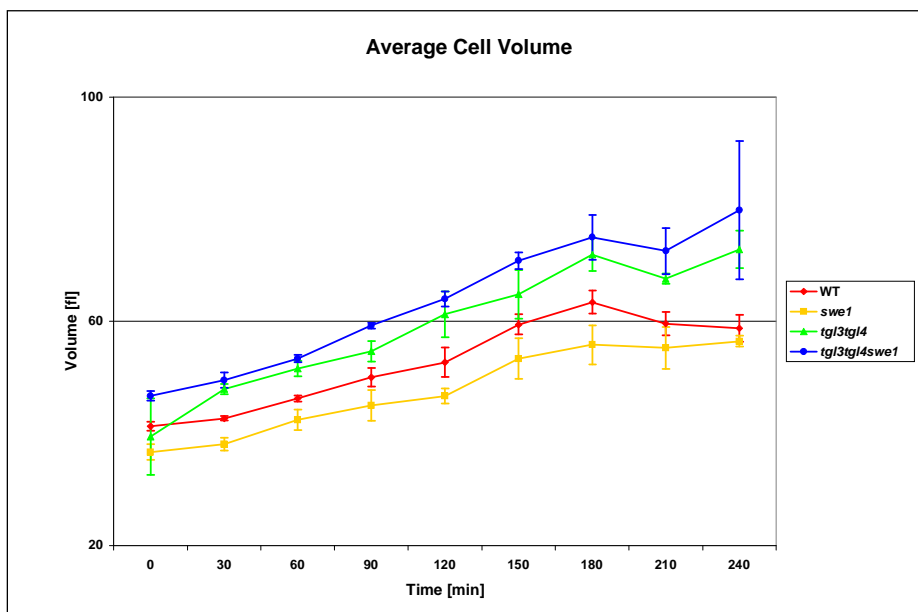


Figure 5.1: Cell volume in the 4 deletion strains over the first 240min after initiation of the cell cycle.

5.3. FACS: Fluorescence activated cell sorting

FACS analysis was used to determine the complete sets of chromosomes in the cell and by this track the cells progression through its division cycle. The first peak represents cells with one full set of chromosomes (1n). Cells have not entered the S-phase of the cell cycle. The second peak that appears represents cells with 2 sets of chromosomes (2n). Those cells have already passed the S-phase and possess 2 identical sets of chromosomes.

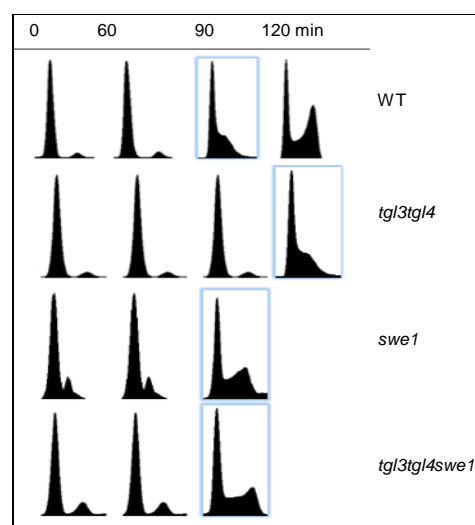


Figure 5.2: FACS analysis of WT and the *swe1*, *tgl3tgl4*, *tgl3tgl4swe1* mutants (courtesy of N. Chauhan).

It should be mentioned that the FACS data shown in **Figure 5.2** was generated from different cultures. This was due to technical problems with the FACS machine during the time the lipid profiling experiments were performed. However as this FACS experiment has been performed many times, and was reproducible, so it will be assumed (only for the purpose of this thesis), that the FACS experiments depicted above are accurate.

WT cells start replicating their DNA between 60 and 90min. The same applies to the *swe1* and the *tgl3tgl4swe1* mutants. The *tgl3tgl4* strain shows a delay of about 30min compared to the other strains, consistent with previous studies. The delay seen in the *tgl3tgl4* strain might be explained by the severely impaired TAG degradation. As a consequence PL production for membranes would be significantly slowed. This delays the whole cell division cycle, as the cells need a certain amount of PL to produce membranes for the emerging daughter cell.

5.4. Cell cycle results for WT and the *swe1*, *tgl3tgl4* and *tgl3tgl4swe1* mutants

The following section will show the obtained results and observations made. For every class of lipids there will be a general graph showing the levels of this lipid class for the 4 deletion strains during the first 240 minutes after initiation of the cell cycle. Additionally to that there will be graphs showing the behaviour of each species within that lipid class.

5.4.1. Triacylglycerol (TAG)

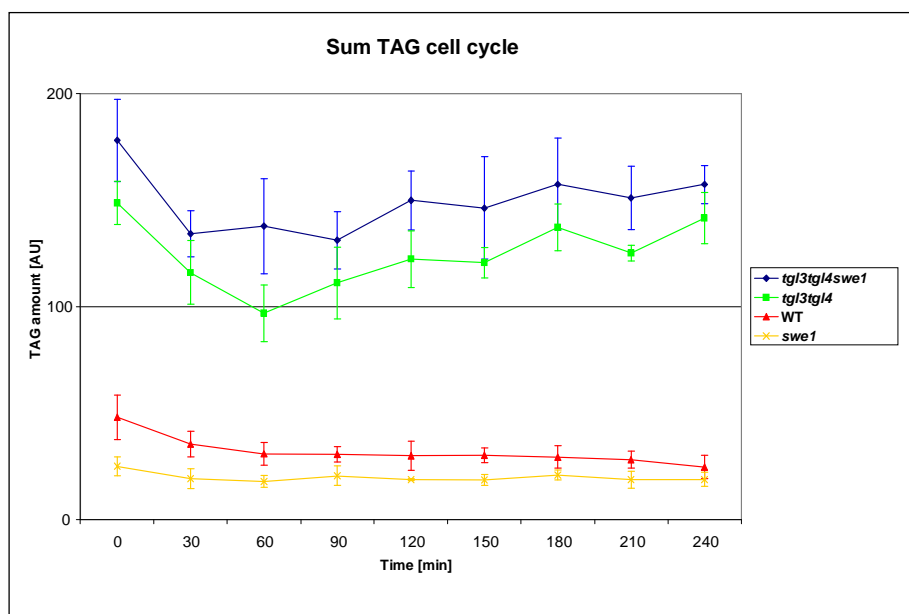


Figure 5.3: Sum TAG in all deletion strains over the first 240min after initiation of the cell cycle.

Figure 5.3 shows the sum of all TAGs in the 4 deletion strains during the first 240min after initiation of the cell cycle. WT TAG levels show behaviour as expected. During the first 60min a decrease of about 36 % can be seen due to TAG mobilisation. TAG being storage molecules are degraded in the first 60min to produce other molecules, such as PL for membrane synthesis. During this period of time TAG degradation is a more energy efficient way to produce PL than “*de novo*” synthesis. In these first 60min it can be assumed that lipolysis outweighs “*de novo*” synthesis, as TAGs are quickly used to produce PL for growth when a new nutrient source is sensed (Kurat et al. 2006, Gray et al. 2004, Zanghellini et al. 2008). After 60min, the total TAG

levels stay constant. There is a dynamic balance between lipolysis and “*de novo*” synthesis. **Figure 5.4** shows that single TAG species vary over time, even if the total TAG amount stays the same.

It was shown during the FACS experiments that WT cells start dividing between 150 and 180min after initiation of the cell cycle. It can be seen in **Figure 5.3** that after 180min the TAG levels start decreasing. This can be partly explained by lipolysis, however it has been suggested that other phenomena might play a role in this TAG decrease, such as the “dilution effect”. The *swe1* mutant shows lower TAG levels than WT. A possible explanation for this might be found in the Swe1p amino-acid sequence. Swe1p shows an acyltransferase motif. If this motif represents a TAG synthesising acyltransferase activity, then Swe1p contributes directly to total lipid levels and the deletion of *SWE1* will decrease total TAG levels. This theory however does not explain the higher TAG levels in the *tgl3tgl4swe1* mutant strain. In the *swe1* mutant the first 60min show a decrease in total TAG levels of roughly 28 %. The slightly lower percentage of decrease might be explained by the smaller cell size of the *swe1* mutant. Less PLs need to be synthesised. FACS and cell counting experiments also suggest that cells in the *swe1* mutant start dividing at a slightly smaller size than WT. A possible explanation for the small cell size is that there is no Cdc28 phosphorylation by Swe1p. Phosphorylated Cdc28p arrests or delays cell division until certain requirements such as cell size are met. When it is not phosphorylated, it can be considered active and cells will divide without having reached a certain size (Lew, 2003).

The *tgl3tgl4* strain shows a permanently increased TAG level. This is due to the missing lipases Tgl3p and Tgl4p. TAGs are not so efficiently degraded and accumulate. However when observing the behaviour over time, the *tgl3tgl4* mutant shows an unexpected decrease in total TAG levels of about 35 % in the first 60min after initiation of the cell cycle. This TAG degradation might be explained by the presence of an additional lipase, such as Tgl5p or Tgl1p for example. Unpublished data (N. Chauhan) shows that Tgl5p is not up regulated on the mRNA level, its activity however could still be amplified. At this time it is hard to say what enzyme is responsible for this TAG decrease in the *tgl3tgl4* strain. This data is unexpected considering previously obtained data (B. Weberhofer, Diploma Thesis 2010). In that case TAG levels increased in the first 3 hours after initiation of the cell cycle. However this should be considered with caution as the culturing conditions were very different. It is known that Tgl5p is present; however this lipase

cannot recover the delay observed in the *tgl3tgl4* strain. It can therefore be postulated that the delay observed in this strain is due to the absence of Tgl3p or Tgl4p.

The *tgl3tgl4swe1* deletion strain shows slightly elevated TAG levels in comparison to the *tgl3tgl4* mutant. The *tgl3tgl4swe1* mutant also shows a decrease in total TAG levels of about 23% in the first 60min, again suggesting the presence of active lipolytic enzymes. Neha Chauhan suggested the idea that Swe1p might be a lipid sensor, and by sensing the lack of lipolysis (or the given products) it delays the cell cycle. Additional deletion of *SWE1* and the subsequent recovery of this delay give circumstantial evidence that this theory might be valid.

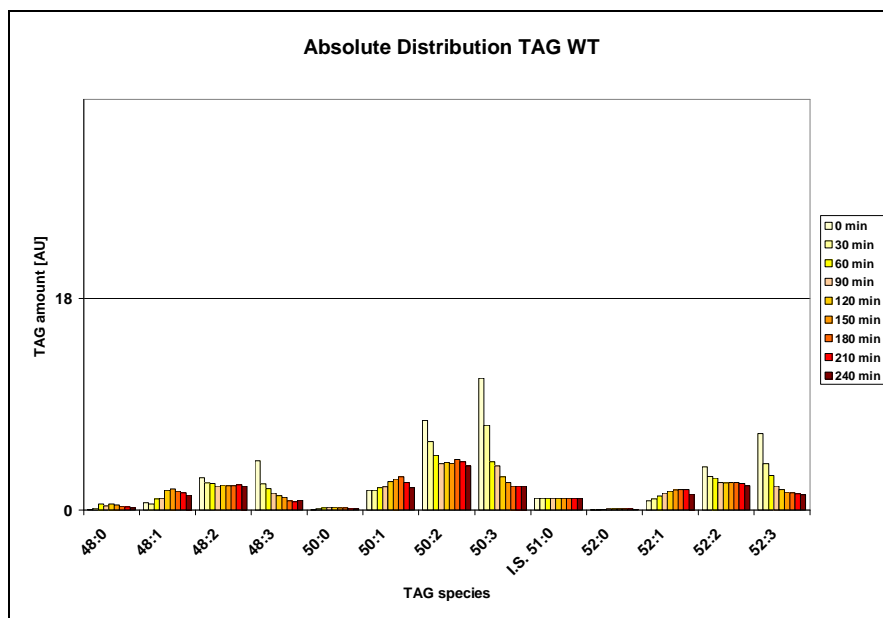


Figure 5.4: Main TAG species observed in WT in the first 240min after initiation of the cell cycle.

Figure 5.4 shows the main species for the WT strain. The main species are TAG 48:0, 48:1, 48:2, 48:3, TAG 50:0, 50:1, 50:2, 50:3, TAG 52:0, 52:1, 52:2, 52:3, and the following discussion will mainly refer to these species. The WT profile can be easily explained when one thinks of the FA composition of these TAGs. The most abundant FAs are 16:0, 16:1, 18:0 and 18:1. **Table 5.1** shows the FA composition of the main TAG species found in WT.

At 0min the main species are double and triple unsaturated TAG species (**Figure 5.4**). The 0min time point is equivalent to a 7 day old culture. It is thought that during quiescence the cells use

TAGs as an energy source (Gray et al., 2004). They use the FA as a substrate for β -oxidation. β -oxidation requires additional steps to degrade unsaturated FA. This explains the higher levels of unsaturated TAG species at the starting time point, as saturated FA may be preferentially used during quiescence to provide energy.

TAG	FA composition			
48:0	16:0	16:0	16:0	0 FA unsaturated
48:1	16:0	16:0	16:1	1 FA unsaturated
48:2	16:0	16:1	16:1	2 FA unsaturated
48:3	16:1	16:1	16:1	3 FA unsaturated
50:0	16:0	16:0	18:0	0 FA unsaturated
50:1	16	16	18	1 FA unsaturated
50:2	16	16	18	2 FA unsaturated
50:3	16:1	16:1	18:1	3 FA unsaturated
52:0	16:0	18:0	18:0	0 FA unsaturated
52:1	16	18	18	1 FA unsaturated
52:2	16	18	18	2 FA unsaturated
52:3	16:1	18:1	18:1	3 FA unsaturated

Table 5.1: FA composition of the main TAG species in WT (FA order cited does not refer to sn-position).

The profile seen in **Figure 5.4** also provides insight as to which species are degraded preferentially over time and which ones are used more for storage. This discussion will relate mainly to the 48:n, 50:n and 52:n species. Species that have no or one unsaturated FAs tend to increase over time. They will be referred to as n:0 and n:1 species, with 0 and 1 referring to the number of double bonds, or more precisely, the number of unsaturated FA in the TAG species. This increase continues until 150-180min, the point where the cells start dividing. (Note that for better visibility **Figure 5.4**, **Figure 5.6**, **Figure 5.7**, **Figure 5.8** do not show error bars which are typically in the range of 10-20%). In the same time range double and triple unsaturated TAG species decrease dramatically. N:2 species decrease most in the first 90-120min, and then seem to stay constant. N:3 are the main species that are degraded. They decrease over time until the cells start dividing. When considering **Figure 5.5** it can be seen that when n:2 and n:3 species are degraded, single and double-unsaturated DAGs are formed. These products are also reflected in the PL composition. The decrease seen in n:2 and n:3 TAG species is also reflected in the DAG, PA and PL profiles (PL 32:n, 34:n, 36:n).

As shown in previous work (Kurat et al., 2009, B. Weberhofer, Diploma Thesis 2010) the main lipases are Tgl3p and Tgl4p. It has been suggested that the preferences of these lipases lie more in the length of the FAs, as opposed to their degree of saturation (Daum et al., 2007). However this could not be confirmed by these experiments. The huge decrease in n:3 TAG species cannot be directly seen in the corresponding DAG profiles. DAGs are intermediary molecules and quickly funnelled towards production of other lipid species. In addition to this DAGs are also bioactive molecules and their levels are strictly regulated (Bielawska et al., 2001).

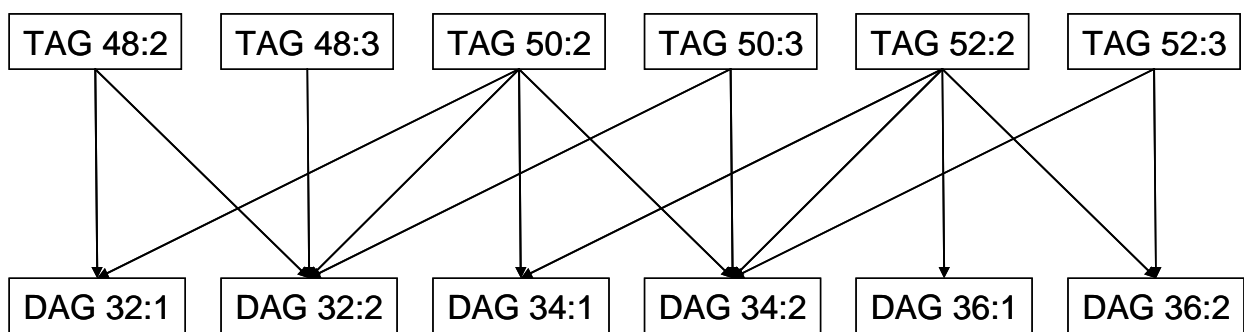


Figure 5.5: TAG degradation and resulting DAG products.

TAG 50:3 and TAG 52:3 are the main species in WT at 0min with both of them constituting about 38% of total TAG amounts. TAG 50:3 is the main species at 0min (equivalent to 7 day old culture). This species represents by itself almost 24 % of the total TAG amount. At 7 days the cells are in quiescence and do not divide anymore. Their membranes do not need to be as dynamic and fluid, so the unsaturated FAs are stored as TAGs (Henry et al. 2011). When the cells are released in new media, they exit quiescence and start dividing again. It has been reported (Dowhan, 1997) that certain species change their membrane composition in response to a change in growth conditions. A possible theory that emerges from this idea is that the membranes of dividing cells need different physical properties to be able to allow bud formation and division. Membrane fluidity for instance is conferred by unsaturated FA in the PL. After about 180min, TAG 50:3 represents only about 7 % of the total TAG amount, suggesting that this species plays an important role during cell division. The degradation products end up in PL, as peroxisomal β -oxidation is repressed when cells exit quiescence (Trotter, 2001).

Figure 5.6 shows the distribution of TAG in the *swe1* strain. The main species distribution is similar to WT with TAG 48:n, 50:n, and 52:n being the predominant species. The levels of these species are slightly lower than those observed in WT. Considering the link between Swe1p, Cdc28p and Tgl4p (introduction), it can be postulated that in absence of Swe1p, Cdc28p stays active and continues to stimulate Tgl4p. This leads to an increased lipolysis and to generally decreased TAG levels. TAG 50:3 and TAG 52:3 are the most important species at 0min with 30% and 18%, respectively, of the total TAG amount. These two species alone constitute almost half of all TAGs in the *swe1* strain. In WT this percentage only amounts to 38%. The main differences compared to WT are that the total levels are slightly lower, that the n:2 species are not degraded over time and that the main species TAG 50:3 and TAG 52:3 represent nearly 50% of the total TAG amount.

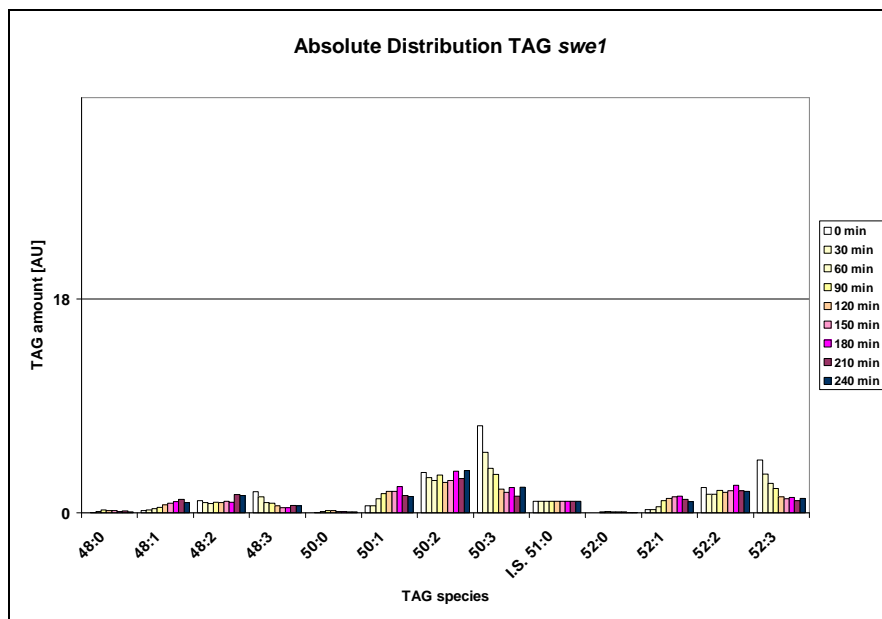


Figure 5.6: Main TAG species observed in the *swe1* mutant in the first 240min after initiation of the cell cycle.

Figure 5.7 shows the distribution of TAG in the *tgl3tgl4* deletion strain. Similar to WT, the main species appear to be TAG 48:n, 50:n and 52:n. However in the *tgl3tgl4* mutant the main species at 0 min seems to be the n:2 species (when compared to n:1 and n:3), as opposed to WT and the *swe1* mutant, where the main species seem to be n:3.

In the *tgl3tgl4* mutant TAG levels are about three times as high as in WT. It shows an increase in very long chain TAGs, such as TAG 58:1, 58:2, 60:1, 60:2, 62:1 and 62:2 (Data not shown). However the percentage they represent of the total TAG amount does not differ significantly from WT. When observed over time however, a different behaviour emerges. Referring to **Figure 5.3**, a major decrease can be seen in the total TAG amount in the *tgl3tgl4* strain in the first 60min after initiation of the cell cycle. This decrease can be seen in nearly all the species. This suggests that the lipolytically active enzyme present does not show a preference for triple unsaturated species as seen in WT. Tgl5p may be important for this degradation, even though it was reported that this lipase shows a substrate preference for C26:0 FA (Daum et al., 2007).

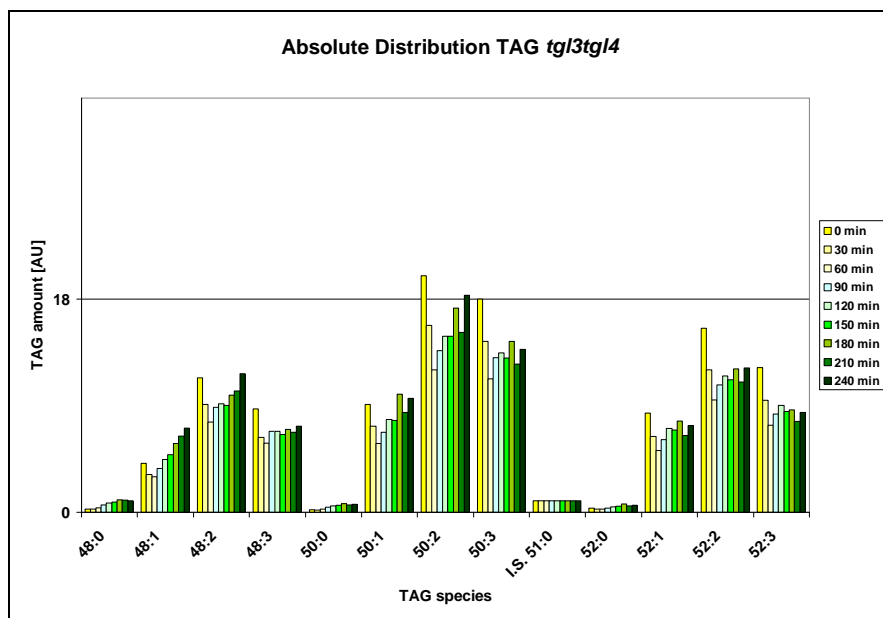


Figure 5.7: Main TAG species observed in the *tgl3tgl4* mutant in the first 240min after initiation of the cell cycle.

As stated before, Tgl5p does not seem to be up regulated on the mRNA level. Its activity could still be increased to compensate for the loss of Tgl3p and Tgl4p. B. Weberhofer suggested in his Diploma Thesis that Tgl5p allows normal growth in the *tgl3tgl4* strain. The main differences observed for the *tgl3tgl4* strain compared to WT are that total TAG levels are about 3 fold higher, the main species at 0min are the n:2 species and there is a degradation of TAG in the first 60min after initiation of the cell cycle.

Figure 5.8 shows the TAG distribution in the *tgl3tgl4swe1* deletion strain. Similar to WT the 48:n, 50:n and 52:n species are predominant. However it becomes clear that the n:2 species are the main molecules, when compared to their n:1 and n:3 counterparts. This suggests a shift in the main TAG species when Tgl3p and Tgl4p are deleted. There are two possible explanations for this: either one of the major lipases Tgl3p or Tgl4p shows preference for n:2 TAG species, and in their absence these species accumulate, or the remaining lipolytically active enzyme, suggested previously, preferentially degrades other species, leaving n:2 levels higher. The additional deletion of *SWE1* in the *tgl3tgl4* strain emphasizes the phenomenon already observed in the *tgl3tgl4* mutant's profile. Observations made in the *tgl3tgl4swe1* strain suggest that Swe1p might have a second link to lipolysis as TAG levels are even higher than in the *tgl3tgl4* mutant. Ubersax et al. (2003) suggest Tgl5p as a potential target for Cdc28p which would explain the TAG degradation in the *tgl3tgl4* and *tgl3tgl4swe1* mutant. However if this were the case, TAG levels in the *tgl3tgl4swe1* mutant should be reduced.

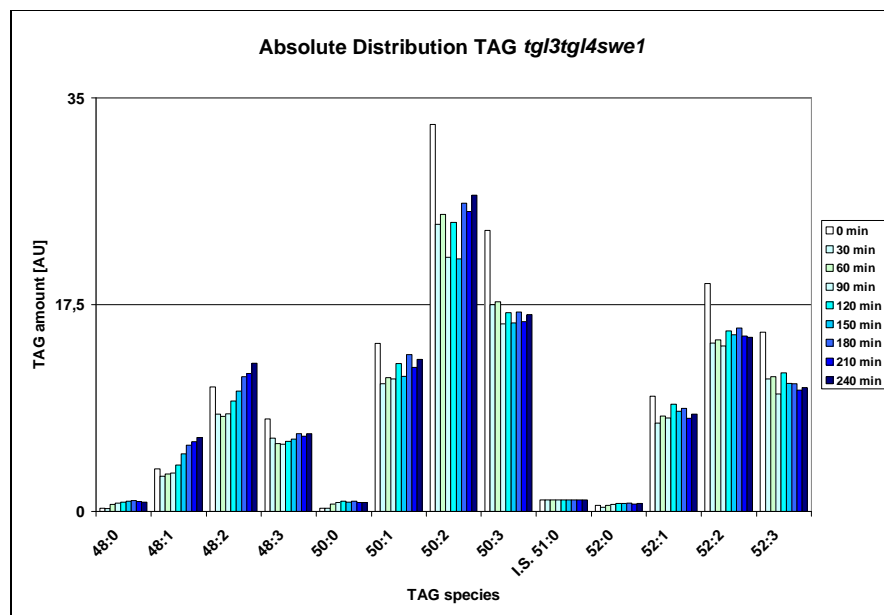


Figure 5.8: Main TAG species observed in the *tgl3tgl4swe1* mutant in the first 240min after initiation of the cell cycle.

Another difference emerges: the *tgl3tgl4swe1* strain only shows TAG degradation in the first 30min. After 30min most TAG species seem to stay stable, or show a slight increase, but not to the same extent as in the *tgl3tgl4* strain. As seen in the *tgl3tgl4* mutant, TAGs containing VLCFA are also increased in the *tgl3tgl4swe1* mutant. However their percentage of the total TAG content is

similar as in WT. The main differences observed for the *tgl3tgl4swe1* strain are higher total TAG levels compared to WT and the *tgl3tgl4* mutant, a clear shift in main TAG species to the n:2 TAGs and a TAG degradation in each species in the first 30min.

5.4.2. Diacylglycerol (DAG)

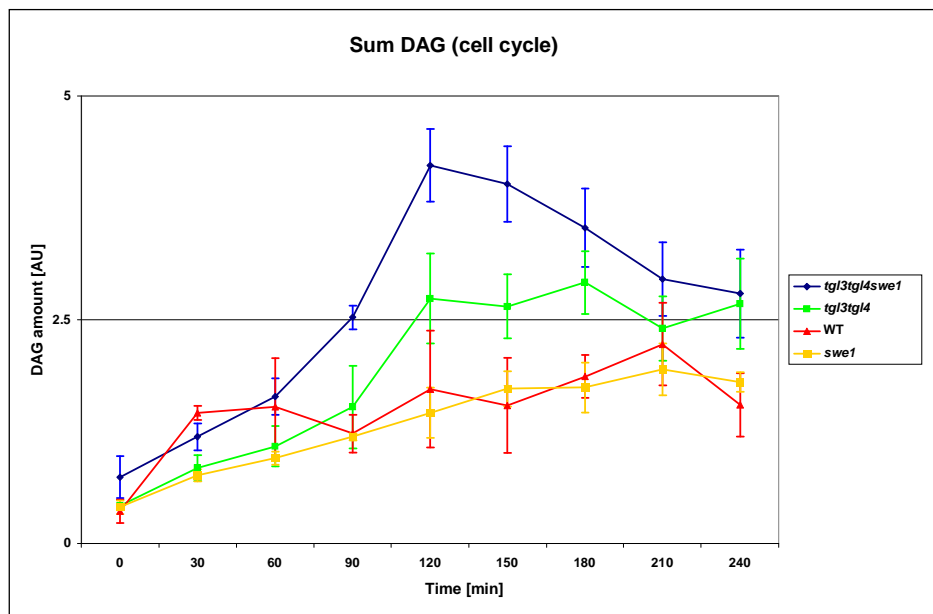


Figure 5.9: Sum DAG in all deletion strains over the first 240min after initiation of the cell cycle.

Figure 5.9 shows the development of DAG in all 4 deletion strains during the first 240min after initiation of the cell cycle. The WT strain shows an initial increase and subsequent decrease in the first 90min that can also be observed in the single species profile (c.f **Figure 5.10**). As budding starts at 90min, this suggests that DAG is involved in this event. After the first 90min, there seems to be a steady increase in DAG species until the cells start dividing. It is hard to relate DAG levels to TAG degradation, as DAG levels are so much lower. DAG is an important intermediate, and it is produced from several different reactions. DAG is also involved in several signalling pathways, so their levels need to be strictly regulated (c.f. **Figure 3.2**). It is hard to draw any tangible conclusions from analysing DAG data from this experiment alone. The *swe1* mutant shows a steady increase of DAG over time. The decrease in DAG levels around 90min observed in WT

disappears. Swe1p has an influence on sphingolipid metabolism, which in turn is also a source of DAG. This might account for the differences between the *swe1* strain and WT.

The *tgl3tgl4* strain shows a pronounced increase in total DAG over the first 120min. This might be due to the TAG degradation, but it is more likely that this increase has to do with signalling. The *tgl3tgl4swe1* strain also shows a high increase in DAG in the first 120min. Again it can be observed that the additional deletion of *SWE1* emphasizes the effect observed in the *tgl3tgl4* strain. An additional observation is that the DAG levels in the *tgl3tgl4* and *tgl3tgl4swe1* mutants end up at similar levels, as do the DAG levels of WT and the *swe1* mutant.

Figure 5.10 shows the distribution of DAG species in the WT strain. In a cell DAG has many different sources, such as TAG degradation, sphingolipid synthesis, phospholipase activity, “*de novo*” synthesis etc. DAG is present in different “pools” and looking at the total amount makes it hard to draw conclusions. **Figure 5.5** suggests that when only considering TAG degradation, one would expect DAG 34:2 to be the most abundant DAG species, as it is a product of the degradation of the main n:3 TAG species. This is not the case, as DAG 34:1 seems to be the quantitatively predominant species (c.f 5.4.4). However qualitatively, considering what TAG species are preferentially degraded, the detected DAG species fit the degradation pattern.

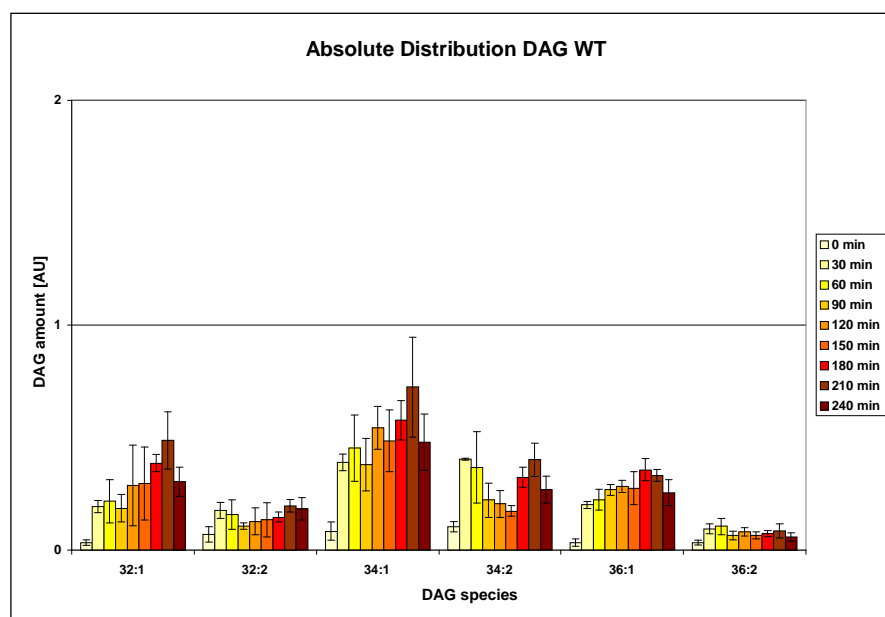


Figure 5.10: Absolute distribution of DAG species in WT over the first 240min after initiation of the cell cycle.

An interesting observation of WT DAG species shows a 0-30min “burst” in DAG. This can be related to the high TAG degradation in that time, but as DAG is also involved in signalling, it is not unlikely that that sudden increase plays a role in the cells leaving the stationary phase. Another interesting observation is that certain species behave in a different way than others. Monounsaturated DAGs behave differently than diunsaturated DAGs, a feature that will be observed in many other lipid species. This suggests very different roles for lipid species with varying FA compositions. Preliminary observations in our lab suggest a different role of monounsaturated versus diunsaturated species (Hofbauer H., Schopf F., Cristobal A.).

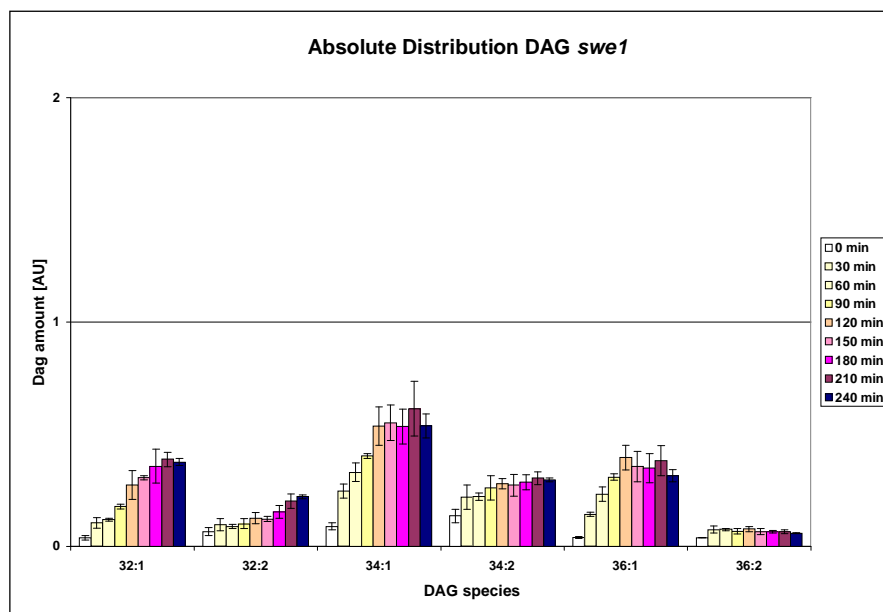


Figure 5.11: Absolute distribution of DAG species in the *swe1* mutant over the first 240min after initiation of the cell cycle.

Figure 5.11 shows the distribution of the different DAG species over time in the *swe1* strain. It reflects the general observation made with the total DAG amounts in WT. At 0min the n:2 species are higher than their n:1 counterparts, however it emerges quickly that n:1 levels get higher than their n:2 counterparts over time. All species increase over time. The *swe1* strain also does not show that 0-30min “burst” as observed in WT. If that sudden increase is due to TAG degradation maybe that suggests that mobilisation in the *swe1* strain is not as pronounced as in WT. As Swe1p is linked indirectly to Tgl4p and its activity through Cdc28p, maybe the absence of Swe1p, and resulting higher lipolytic activity of Tgl4p, may explain the steady increase of DAG over time.

However since the levels are so low, they cannot be directly correlated to the degraded TAGs without further study.

Figure 5.12 shows the distribution and development of DAG in the *tgl3tgl4* strain. The n:1 species behave differently than the n:2 species. n:1 species show a clear increase until 120min, and then they level out. This might be linked to TAG degradation during this time. n:2 species stay constant until 90min and then show an increase, suggesting n:2 are quickly used for something else. All species show a “burst” between 90-120min, suggesting a link to the budding behaviour of the *tgl3tgl4* strain.

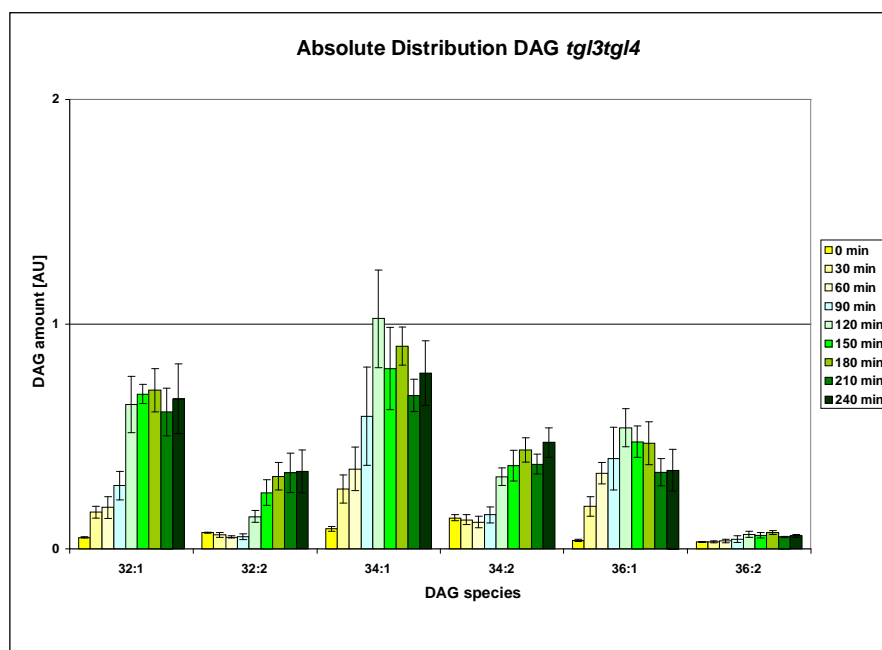


Figure 5.12: Absolute distribution of DAG species in the *tgl3tgl4* mutant over the first 240min after initiation of the cell cycle.

Figure 5.13 shows the development of DAG species in the *tgl3tgl4swe1* strain. The behaviour of the DAG species is similar as in the *tgl3tgl4* mutant; again it is emphasized by the additional deletion of *SWE1*. n:1 species show an increase until 120min, and then a clear decrease. This could partially be linked to TAG degradation during this time period. However the total TAG amounts only show a TAG degradation during the first 30min, suggesting that additionally to that DAG in this strain originates from other sources. DAG 34:1 shows a 10 fold increase over the first 120 minutes. This correlates to the fact that TAG 50:2 is the main species in this strain. The n:2 species

decrease in the first 30min suggesting that these species are actively used from the beginning of cell cycle initiation.

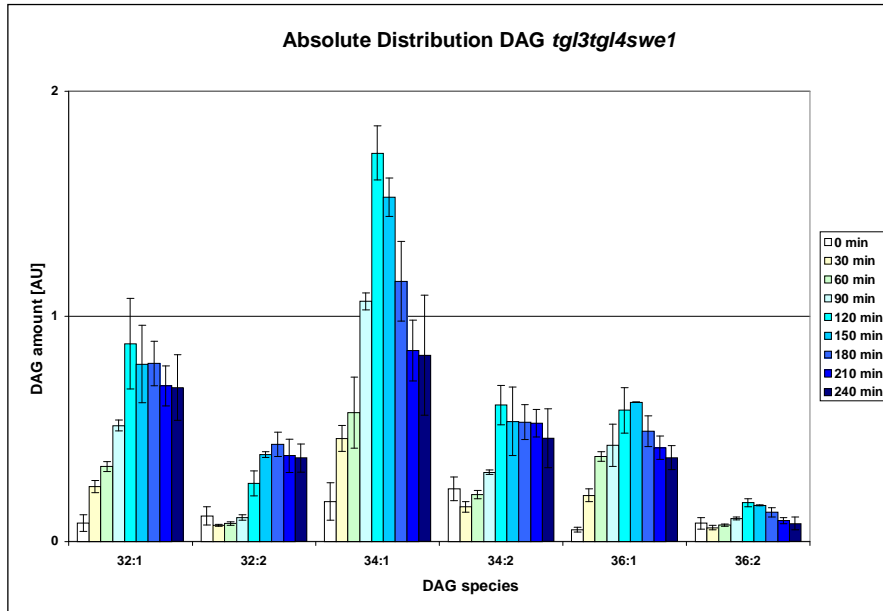


Figure 5.13: Absolute distribution of DAG species in *tgl3tgl4swe1* mutant over the first 240min after initiation of the cell cycle

5.4.3. Phosphatidic acid (PA)

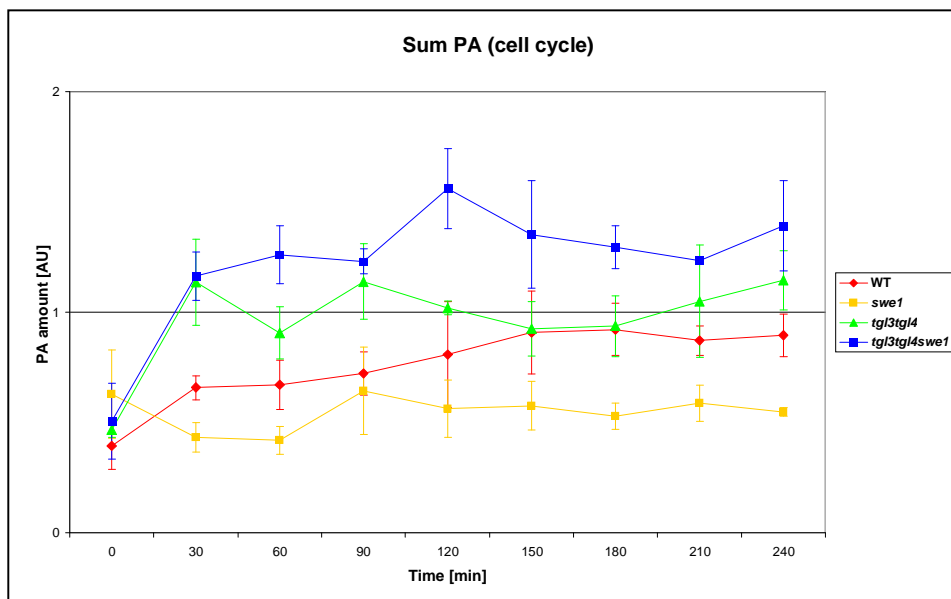


Figure 5.14: Sum PA in all deletion strain over the first 240min after initiation of the cell cycle.

Figure 5.15 shows the PA distribution and development over time in the WT strain. PA 32:1 and PA 34:1 are the predominant species. They show a steady increase until the cells start dividing. PA 32:2 and PA 34:2 show a significant increase in the first 30min, suggesting these species play a role in budding. PA levels are very low, which reflects the fact that PA is a tightly regulated intermediary molecule and is very quickly funnelled into PL or even neutral lipid production. n:1 species are always higher than their n:2 counterparts. DAG 34:1 And PA 34:1 end up mainly in PI (**Figure 5.20**). The equivalent 34:2 species appear to end up more in PS, PE and PC.

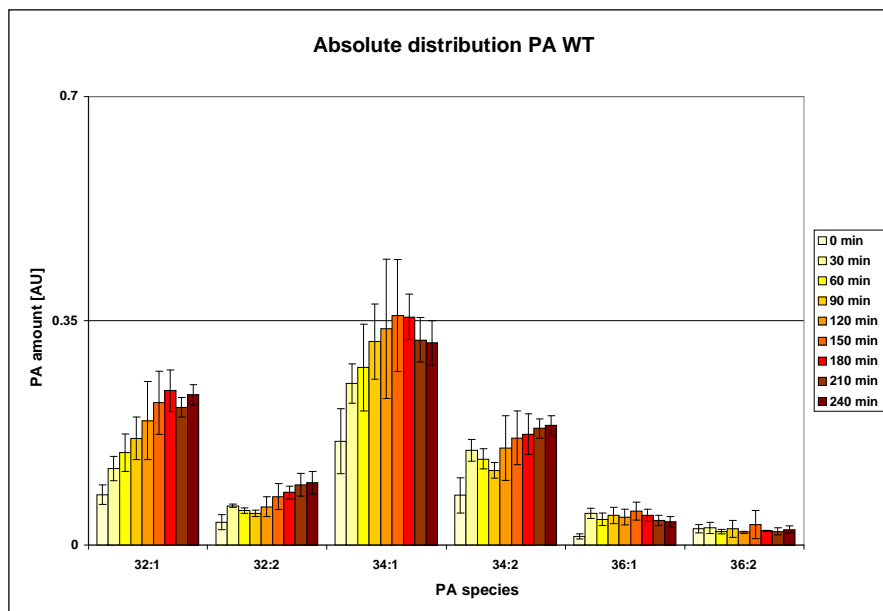


Figure 5.15: Absolute distribution of PA species in WT over the first 240min after initiation of the cell cycle.

Figure 5.16 shows the distribution of PA in the *swe1* deletion strain. The profile is very different to the one seen in WT. PA 32:1 is not present at the same amounts as in WT. The behaviour observed in **Figure 5.14** during the first 90min is also seen here in the main species 32:n and 34:n. PA 32:2 and 34:2 species only decrease in the first 30min and then increase until 90min. After that it is unclear whether they stay constant or decrease. This indicates that these species might serve as substrates for PL production. An interesting aspect is the 0-30min decrease in the main species 32:n and 34:n. This is in stark contrast to what is observed in WT. The reason for this decrease is still unclear. As Swe1p is also involved in sphingolipid metabolism, and PI serves as a precursor for some of these molecules, it can be assumed that n:1 PA species might be directed towards this

pathway. **Figure 5.20** which depicts PI levels in the *swe1* strain gives credibility to this claim as the PI 34:1 species shows a related increase during the first 30min. An analysis of spingolipid levels would confirm this claim.

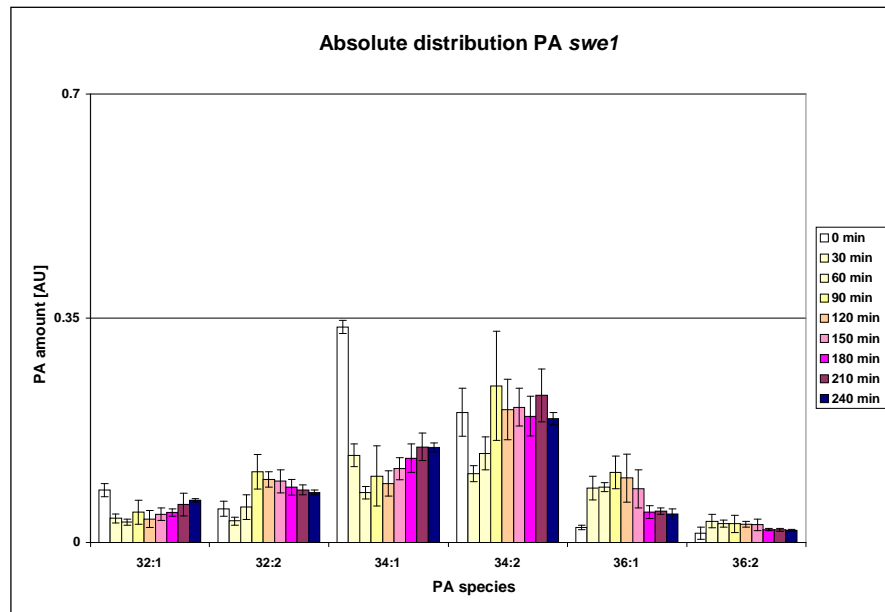


Figure 5.16: Absolute distribution of PA species in *swe1* over the first 240min after initiation of the cell cycle.

The PA 32:1 species is higher in all other deletion strains. DAG 32:1 and PA 32:1 are most likely products of TAG 48:2 and TAG 50:2 degradation. Referring to **Figure 5.6** and the observation that the main TAG n:2 species stay relatively constant over time, the fact that PA 32:1 is so low in the *swe1* strain is a logical consequence.

Figure 5.17 shows the distribution of PA in the *tgl3tgl4* strain. The pattern observed for the PA species is very different to that of WT or the *swe1* strain. PA 32:1 and 34:1 are the predominant species; just like in WT, however their behaviour differs. They show a sharp increase in the first 90min, which can be explained by the TAG degradation during that time or even increased “*de novo*” synthesis. PA 32:2 and PA 34:2 show a similar pattern to each other. They peak at 30min suggesting they are quickly synthesised after the G0 exit and that reactions that use these species only start up a little later. If the theory mentioned earlier is correct, and the activity of Tgl5p is increased, this could explain certain fluctuations in the PA levels of the *tgl3tgl4* strain, as Tgl5p also shows a PA acyltransferase activity (Rajakumari et al., 2010).

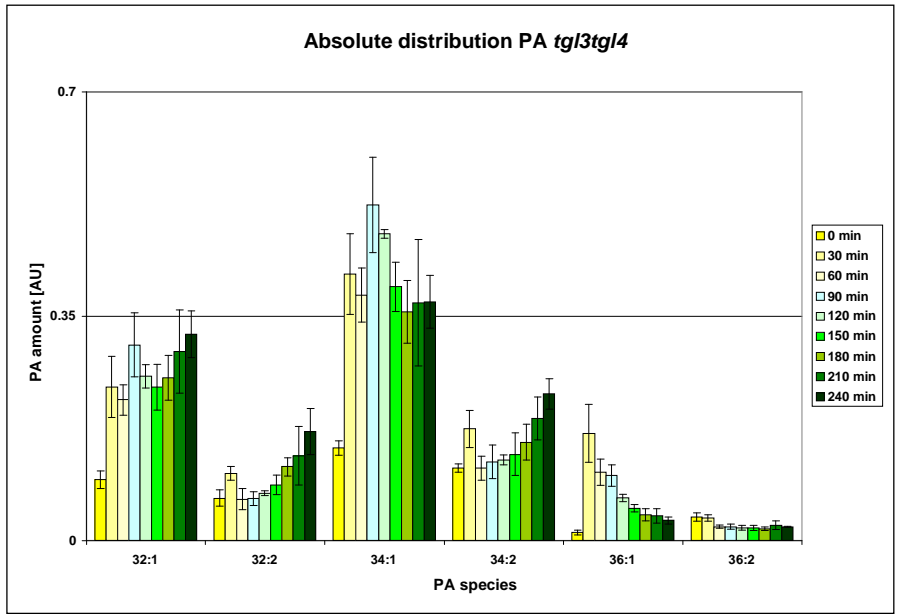


Figure 5.17: Absolute distribution of PA species in *tgl3tgl4* over the first 240min after initiation of the cell cycle.

Figure 5.18 shows the distribution of PA in the *tgl3tgl4swe1* strain. The behaviour is very similar to what was observed in the *tgl3tgl4* strain. The increased amounts that are observed might be due to the increased cell size, or to the additional deletion of *SWE1*.

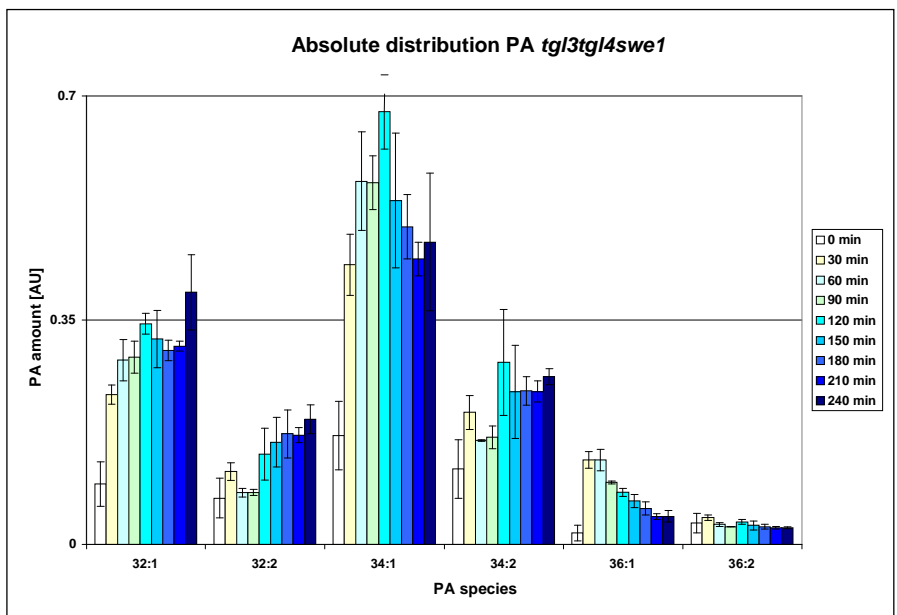


Figure 5.18: Absolute distribution of PA species in *tgl3tgl4swe1* over the first 240min after initiation of the cell cycle

5.4.4. Phosphatidylinositol (PI)

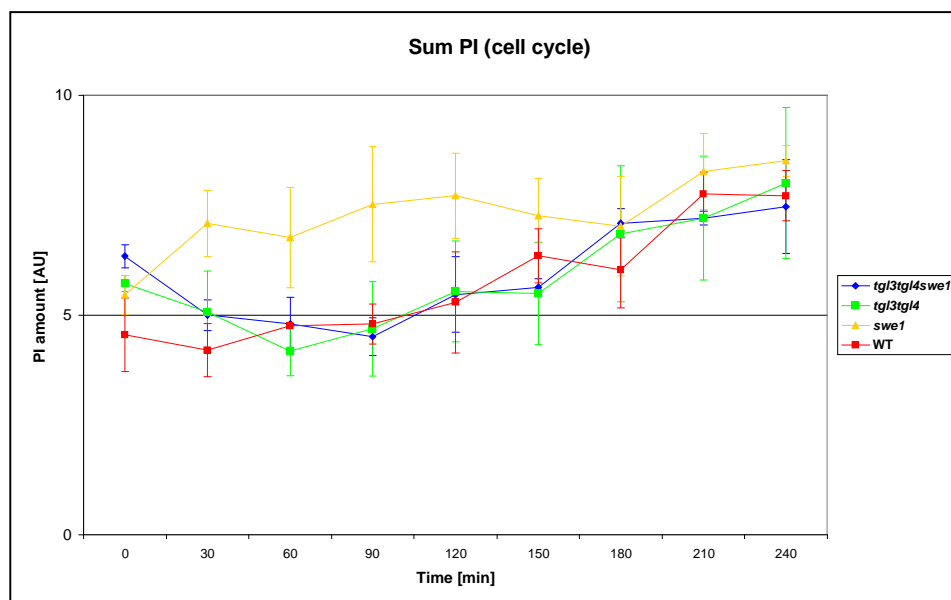


Figure 5.19: Sum PI in all deletion strain over the first 240min after initiation of the cell cycle.

Figure 5.19 shows the development of PI over time in the 4 deletion strains. WT, the *tgl3tgl4* and *tgl3tgl4swe1* mutants develop in a similar way, although the latter two show a pronounced decrease in the first 60min. The *swe1* strain shows higher PI levels during the time where budding plays a role. All 4 strains start at similar levels and end at similar levels, but the development of PI in the *swe1* strain differs over time.

Figure 5.20 shows the typical PI profile in a WT strain. The major species are the n:1 species, and they increase steadily over time. This can be related to the increase of membranes during growth. n:2 species show a different behaviour: they decrease over the first 90-120min and then increase again. PI is also used as a building block for other species, such as PIPs or IPC. This suggests that n:2 species might be used to produce those other molecules, but this needs to be further investigated. An interesting aspect would be to check if PIPs and IPC prefer unsaturated FA as the PI n:2 species are so low. Another explanation could be that they are remodelled into n:1 PI species.

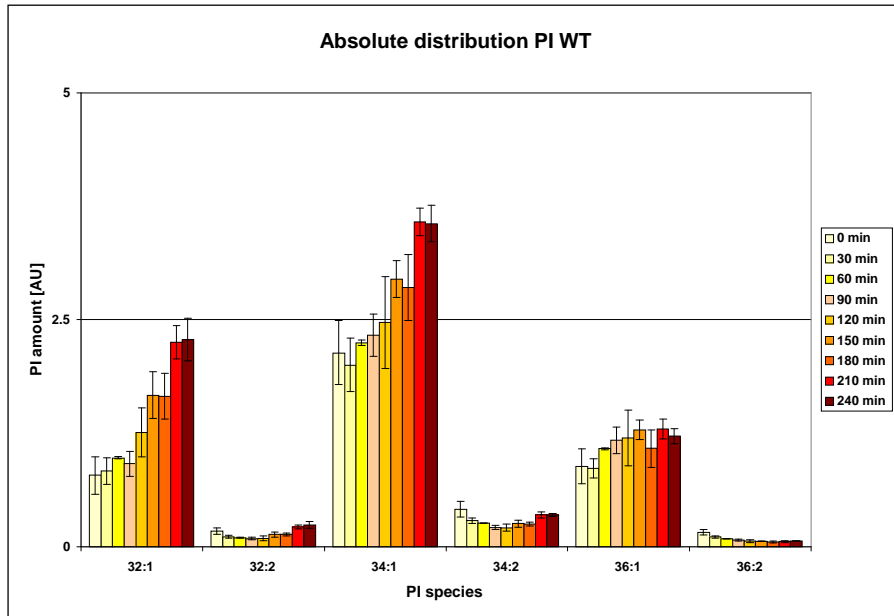


Figure 5.20: Absolute distribution of PI species in WT over the first 240min after initiation of the cell cycle.

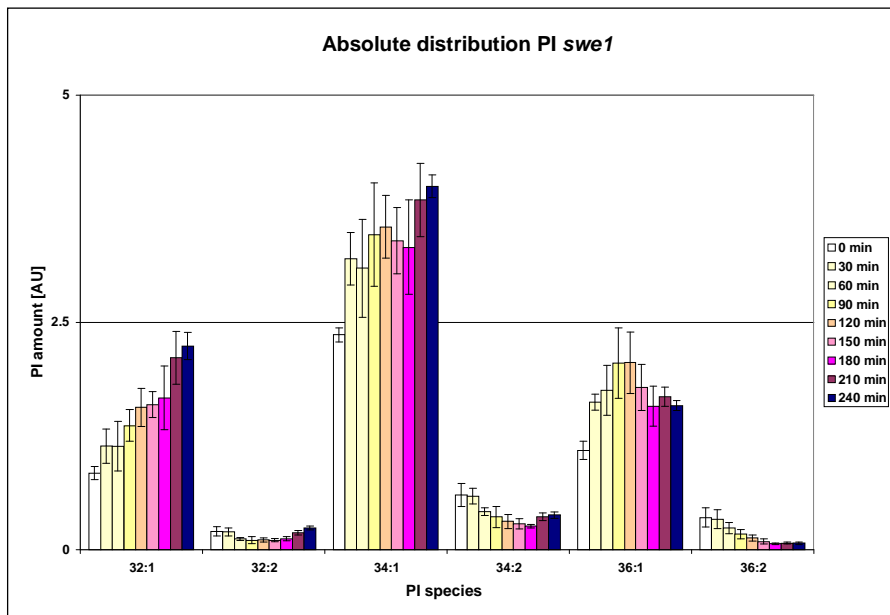


Figure 5.21: Absolute distribution of PI species in *swe1* over the first 240min after initiation of the cell cycle.

Figure 5.21 shows the distribution of PI in the *swe1* strain. The general tendencies are similar to those observed in WT. n:1 is the major species and shows an increase over time which can be linked to growth. The n:2 species also show a similar behaviour, however they seem to reach their minimum level at around 180min, whereas in WT the minimum level seems to be reached at

around 120min. The levels of PI 34:1 and PI 36:1 are higher than those in WT linking these species to the higher total levels of PI seen in the *swe1* strain. This indicates that these species are critical to the differences seen between WT and the *swe1* mutant.

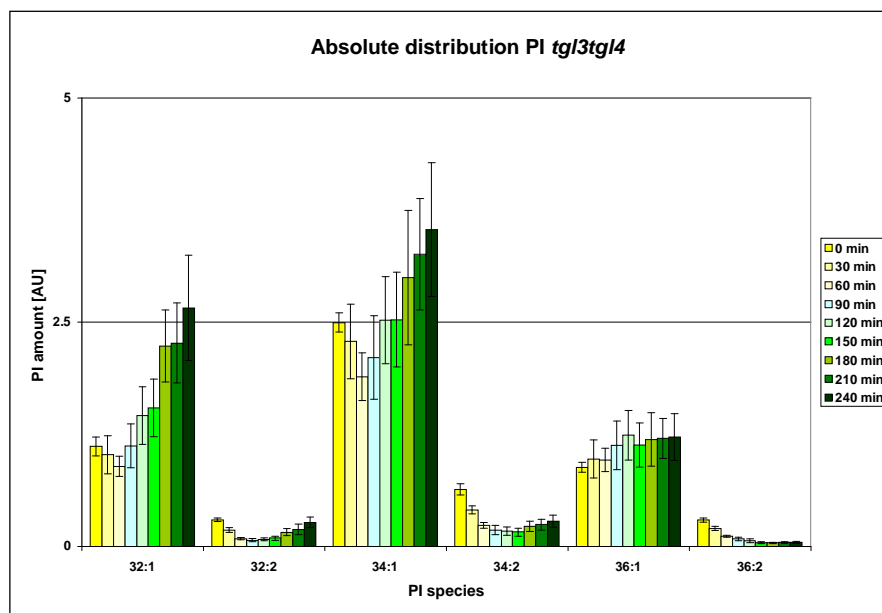


Figure 5.22: Absolute distribution of PI species in the *tgl3tgl4* strain over the first 240min after initiation of the cell cycle.

Figure 5.22 shows the distribution of PI in the *tgl3tgl4* strain. The main species are the same as in WT, namely the n:1 species. Even though they show a general increase over time, PI 32:1 and 34:1 show a surprising decrease in the first 60min. A possible explanation for this drop could be remodelling or maybe they are funnelled into sphingolipid metabolism. The n:2 species show a similar behaviour as in WT, with a decrease until 120min. The profile in the *tgl3tgl4swe1* strain (data not shown) is very similar to that observed in the *tgl3tgl4* mutant, with a difference being that the PI 34:1 species decrease until 90min before rising again and PI 36:1 seems to stay constant rather than increasing.

5.4.5. Phosphatidylserine (PS)

Figure 5.23 shows the development of PS over time in all 4 deletion strain. Even though a high error can be seen, the PS levels in all 4 strains seem to start, develop and end in a similar way.

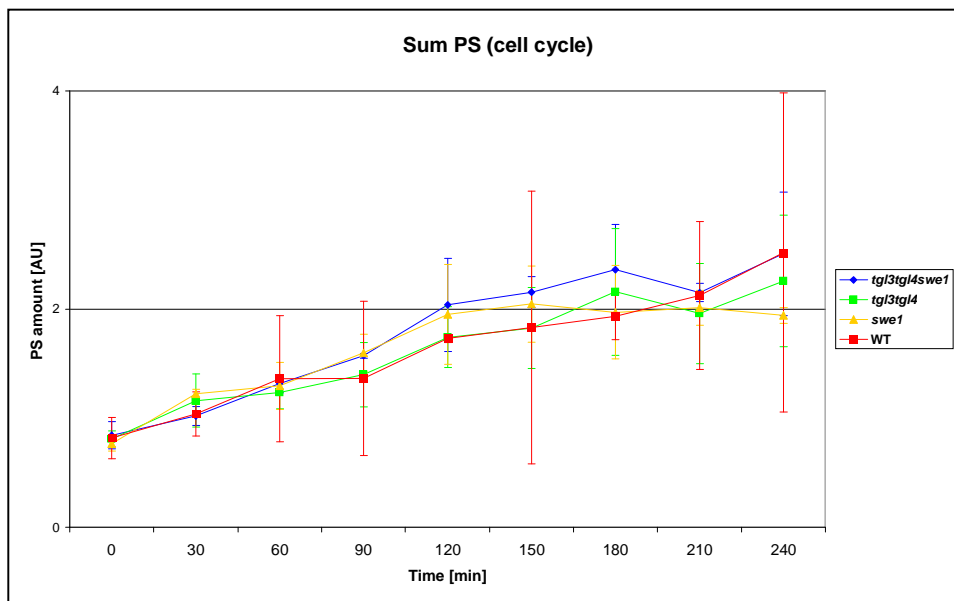


Figure 5.23: Sum PS in all deletion strain over the first 240min after initiation of the cell cycle.

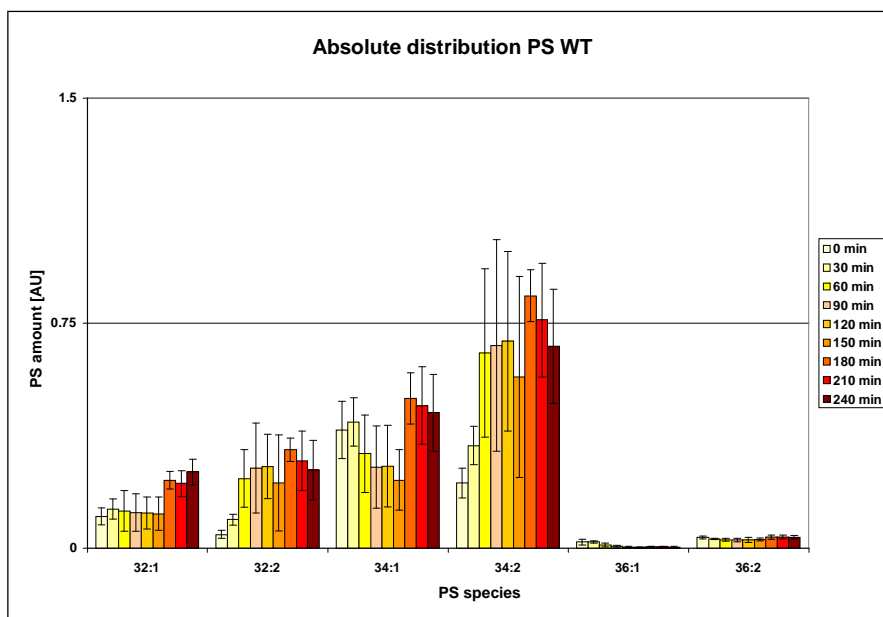


Figure 5.24: Absolute distribution of PS species in WT over the first 240min after initiation of the cell cycle.

Figure 5.24 shows the distribution of PS in WT. The profiles of the *tgl3tgl4* and *tgl3tgl4swe1* strains display minor differences to the WT profile (data not shown). The main species are 32:n and 34:n, with 34:2 standing out at later time points. 36:n species will not be considered in this

section. All species seem to show an increase over time except PS 34:1, which decreases until 150min. This decrease is much less pronounced in the *tgl3tgl4* and *tgl3tgl4swe1* strain, but still present. The *swe1* strain shows a rise in the first 30min for this species. The measurements in this experiment show high errors, and should be considered with caution. The question arises as to what is the fate of this PS 34:1 species? The most likely explanation is that it is remodelled into PS 34:2. PS is a precursor to PE and PC and the main species in these PL are 34:2.

5.4.6. Phosphatidylethanolamine (PE)

Figure 5.25 shows the development of PE over time in all 4 strains. WT and the *swe1* mutant show similar behaviour, both show a decrease in the first 30min, followed by an increase over time. They end up at the same level. The *tgl3tgl4* and *tgl3tgl4swe1* mutants also show similar behaviour although their levels are slightly higher. However the drop observed in the *tgl3tgl4* mutant seems to go on until 60min, whereas all other strains show an increase after 30min. This is the first species that might reflect the 30min delay in the cell cycle observed during the FACS analysis. All of these initial drops could be explained by the fact that PE is also a precursor to PC, a main PL component of membranes and that excess PE is funnelled into PC production.

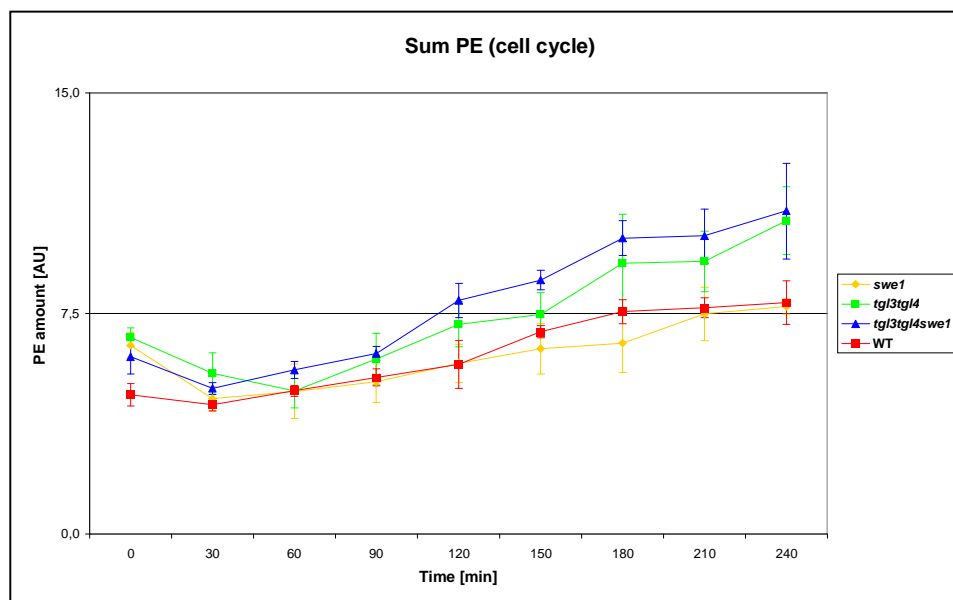


Figure 5.25: Sum PE in all deletion strain over the first 240min after initiation of the cell cycle.

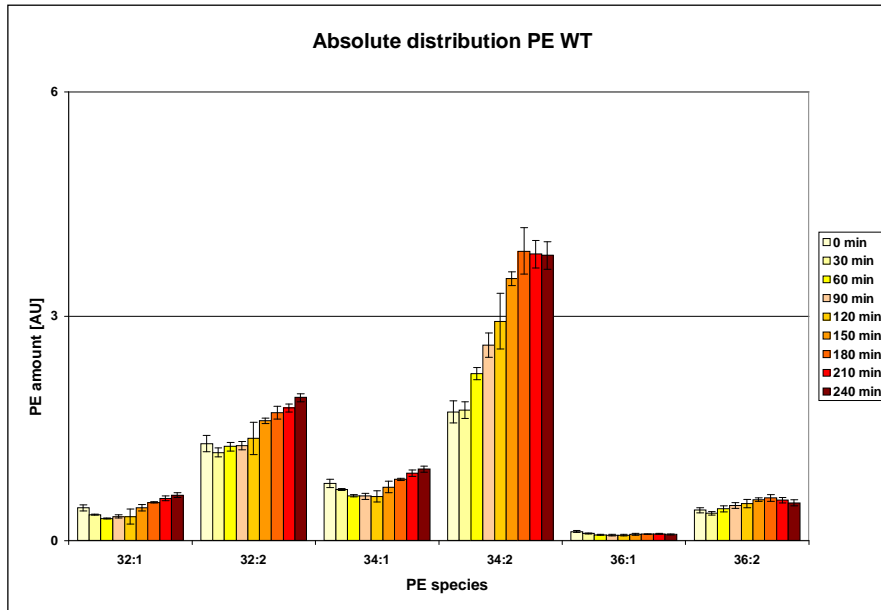


Figure 5.26: Absolute distribution of PE species in WT over the first 240min after initiation of the cell cycle.

Figure 5.26 shows the PE distribution in the WT strain. It is interesting to see that the main species seem to be reversed compared to PI, with PE 32:2 and 34:2 being the major species. Both of them show a steady increase over time although in PE 32:2 a clear increase is only seen after 120min. PE 32:1 and 34:1 show a slight decrease in the first 60min, then they rise again. The minimum level seems to be reached between 60 and 120min. The *swe1* strain shows a similar profile to WT (data not shown). The only differences are that PE 32:2 seems to stay constant over time and that the decrease in the n:1 species is not as pronounced. PE is a major component of biological membranes. A change in level over time of certain PE species might indicate that more or less PE is needed to form membranes. One could argue that in order to bud, the membrane composition needs to change. A different PL composition will give rise to different physical properties required during budding or growth in general.

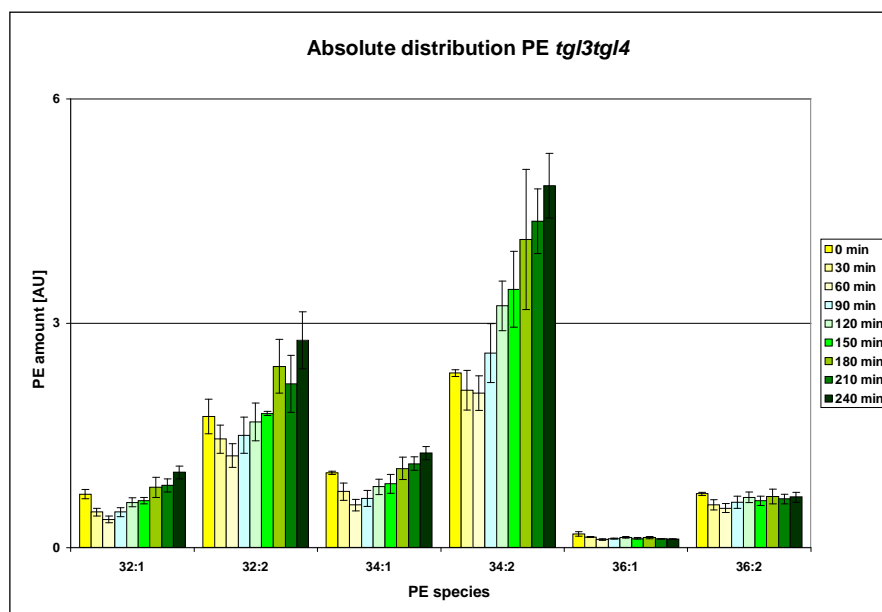


Figure 5.27: Absolute distribution of PE species in the *tgl3tgl4* strain over the first 240min after initiation of the cell cycle.

The *tgl3tgl4* strain (**Figure 5.27**) shows the same main species as WT and the *swe1* mutant, but their behaviour differs. The drop in PE 32:1 and 34:1 only lasts the first 60min but is much more pronounced. The same tendencies can be seen in PE 32:2 and PE 34:2: first a decrease and then a significant increase over time. This might be explained by the fact that PE gets transformed into PC before budding starts. However that would be seen in all strains. The tendencies in the *tgl3tgl4swe1* strain are similar to those observed in the *tgl3tgl4* strain. A notable difference is that the n:2 species start their rise already at 60min. However the n:1 only start increasing after 90min.

5.4.7. Phosphatidylcholine (PC)

Figure 5.28 shows the levels of PC in all 4 deletion strains. WT shows a slight increase over time, however not significant enough to correlate PC content to cell growth. This might be explained by a change of PL composition of the membrane. Unfortunately total PL levels cannot be calculated, as the different PL classes were analyzed using different IST. After 180min PC levels of WT seem to decrease a little, which is logical when considering cell division and decreased cell size. The *swe1* mutant shows a rise until 150min and then a decrease.

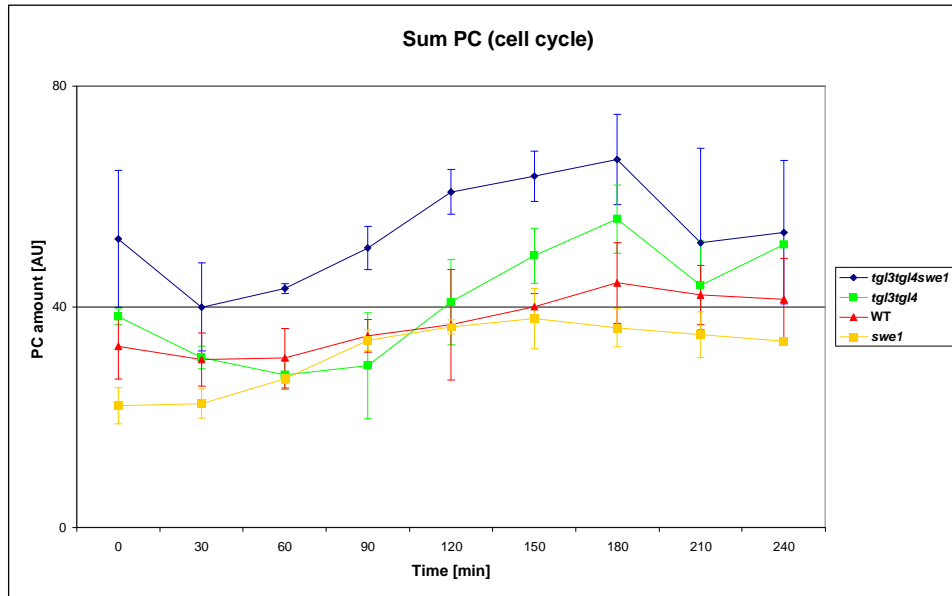


Figure 5.28: Sum PC in all deletion strains over the first 240min after initiation of the cell cycle.

The *tgl3tgl4* strain shows a surprising decrease in the first 60-90min. This might be explained by a change in membrane composition, and PC is used to produce other necessary lipid species. The *tgl3tgl4swe1* mutant shows a decrease in the first 30min, however due to the higher errors this drop should be considered with caution. Both strains show a drop in PC levels after 180min, which can be correlated to the smaller cell size after division. If one would ignore the 0min time point, things might seem more logical. The 0min time point seems to show high errors. This could be due to the fact that the cells were frozen in Tris buffer (as opposed to a rest of media for the other time points). This might still contain a rest of RediGrad solution, which might interfere with the analysis. It is unlikely though, as this would be seen in all other lipid classes. Another explanation might be that at 0min, the cells are stationary. After 7 days they might have a thicker cell wall, which would interfere with the analysis. Again this argument would imply that it would be seen in all classes. Looking at these results in a different perspective, for the first time the delay of the *tgl3tgl4* mutant might be seen. WT and the *swe1* mutant PC levels do not decrease at first. The *tgl3tgl4* mutant PC levels decreases until 60min, and the *tgl3tgl4swe1* mutant's PC levels drop the first 30min. This might illustrate a partial recovery of the delay.

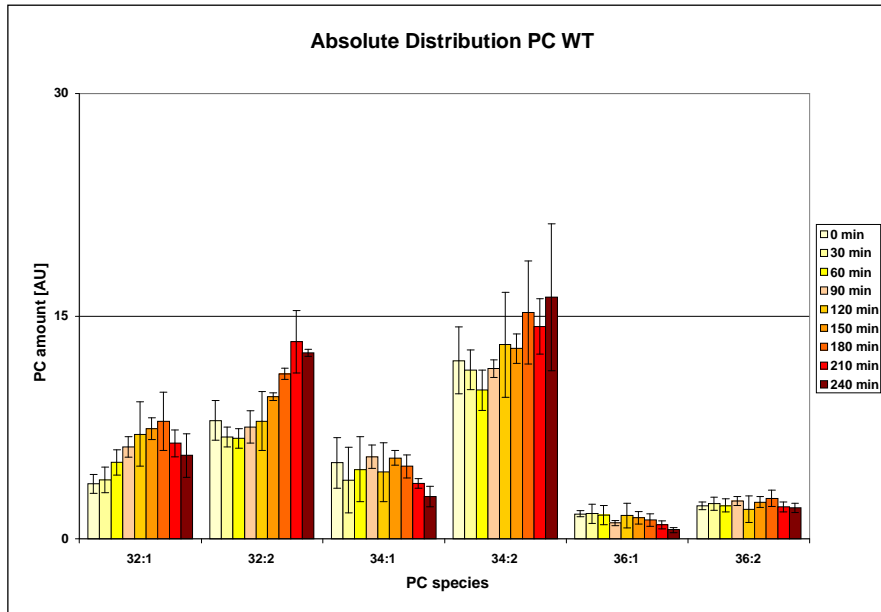


Figure 5.29: Absolute distribution of PC species in WT over the first 240min after initiation of the cell cycle.

Figure 5.29 shows the PC profile in WT. PC 32:2 and 34:2 are more predominant than their n:1 counterparts. PC 32:1 increases until cell division start, whereas PC 34:1 seems to stay relatively constant until cell division. PC 32:2 and PC 34:2 only show a clear increase after 120min. It is unclear if they are constant or if they decrease before that.

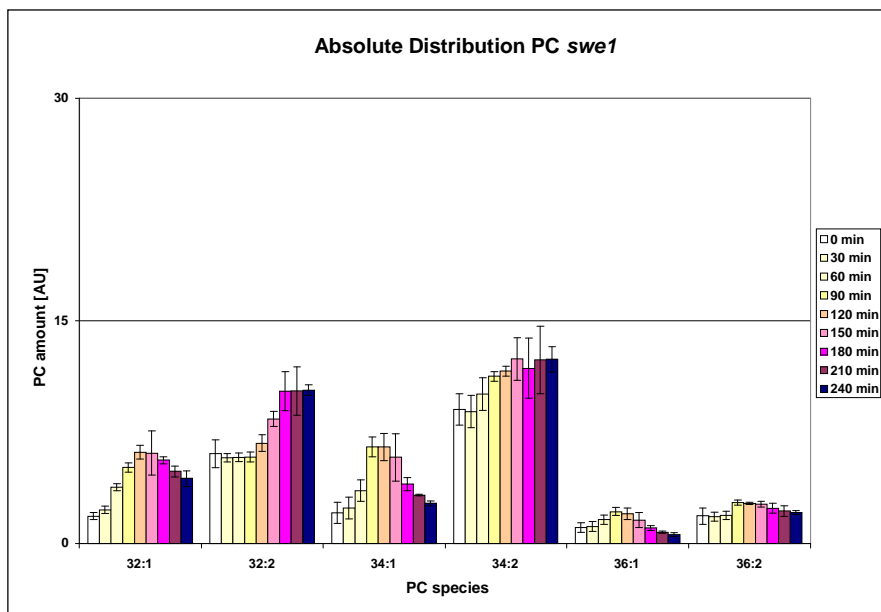


Figure 5.30: Absolute distribution of PC species in *swe1* over the first 240min after initiation of the cell cycle.

The behaviour of PC in the *swe1* deletion strain is very similar to that observed in WT with a few notable differences (**Figure 5.30**). PC 32:1, PC 34:1 and PC 36:1 start their decrease already at 120min, which suggest that certain PC species are not needed after budding. PC 32:2 stays constant until 90min, which suggests that this species becomes significant after budding.

The PC profile of the *tgl3tgl4* strain seen in **Figure 5.31** shows a significant difference to WT and the *swe1* strain. PC 32:2 drops in the first 60min and then rises significantly. PC 34:2 shows a decrease that lasts 30min longer before it rises again. The drop at 90min in PC 32:1 might also be of importance. A possible explanation for this decrease observed in most of the species might be that with TAG degradation gone, PC serves as a source of FA. These FA could be used for remodelling or maybe for protein modification. Phospholipases and other lipases might increase their activity to provide precursors for molecules that are imminently required for cell division. The PC profile of the *tgl3tgl4swe1* strain is very similar to that observed for the *tgl3tgl4* mutant. However the drop observed in the PC 34:2 species only seems to last 60min. This might be an indication that this species is a key player in the delay observed in the *tgl3tgl4* strain.

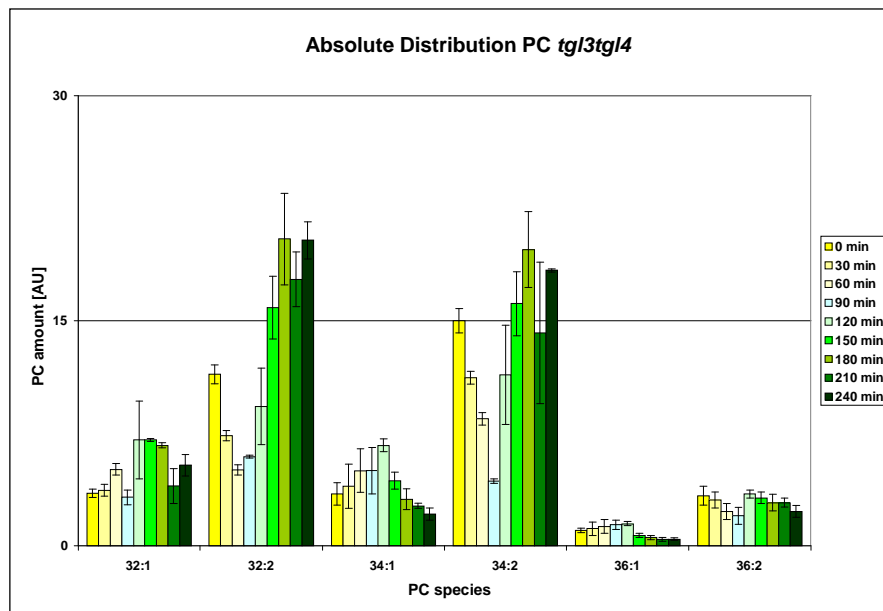


Figure 5.31: Absolute distribution of PC species in the *tgl3tgl4* mutant over the first 240min after initiation of the cell cycle.

5.5. Growth phase results for WT and the *swe1*, *tgl3tgl4*, *tgl3tgl4swe1* mutants

A different set of measurements was taken during the experiments described earlier, to illustrate the behaviour of certain lipid species in the cells beyond the first cell cycle. (c.f.: § 3.2.1). The results of these measurements are shown in the following section. It is important to keep in mind that for all graphs depicted here, the 0h time point is equivalent to a 7 day old culture and that the time point 72h in the *swe1* strain is only represented by a duplicate experiment.

5.5.1. Triacylglycerol (TAG)

Figure 5.32 shows the evolution of the total TAG content in the 4 deletion strains over a time period of 72h. As observed earlier, all strains show a slight decrease of TAG content over the first 3 hours. B. Weberhofer observed a drastic drop in TAG levels in the first 9 hours in most of his strains. He argues that this is due partially to TAG utilisation and partially to the “dilution” effect of cell division. However in these experiments this 9h drop can only be seen in the *tgl3tgl4* strain. It has to be noted though that the culturing conditions in these experiments were very different than those used by B. Weberhofer, which could explain the differences in cell behaviour.

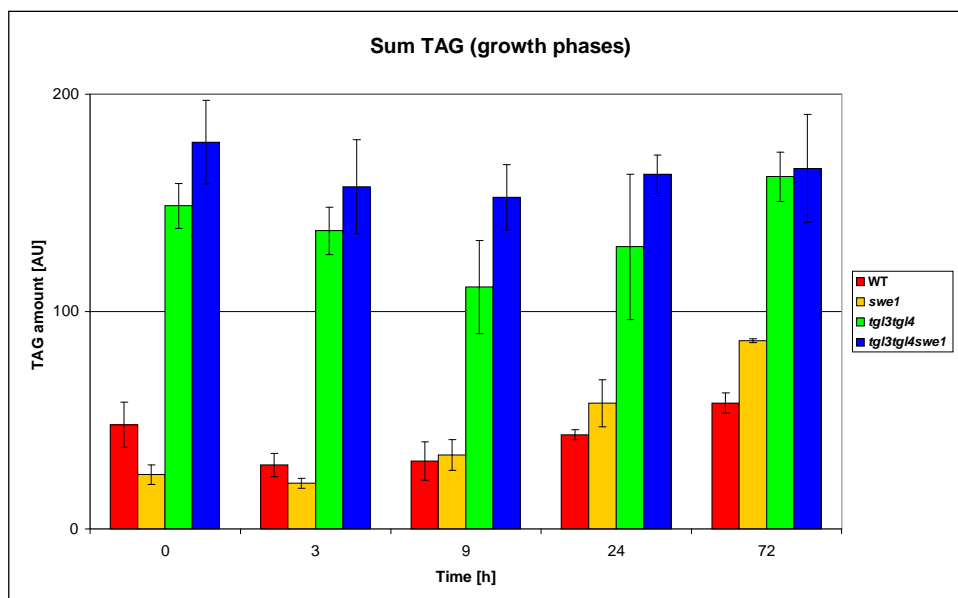


Figure 5.32: Sum TAG in all deletion strains over 72h after inoculation into fresh media.

WT shows a decrease in the first 3h that is discussed in detail in §5.4.1. At 9h the TAG levels are similar to those at 3h. It can be argued that TAG synthesis has started up again, since cells are in their exponential phase, dividing quickly and the TAG levels stay constant. Over time the TAG levels increase to a maximum at 72h. It is interesting to observe that TAG levels at 0h and 72h are not that different. TAG levels are quite dynamic even in the stationary phase.

One observation of the species behaviour does show an interesting aspect: while at 0h the main TAG species seem to be triple unsaturated TAGs, at 72h the double unsaturated TAGs are predominant. This is logical since the cells are quiescent and in absence of an external energy source they degrade TAGs as a source of energy, using FA as substrate for peroxisomal β -oxidation (Gray et al, 2004). Saturated FAs are easier to degrade than unsaturated FA, explaining the decrease in the degree of saturation in TAG over time. (c.f **Figure 5.33**). Between 72h and 7 days (0h) the amount of saturated FA in the total TAG drops from roughly 35% to 21%.

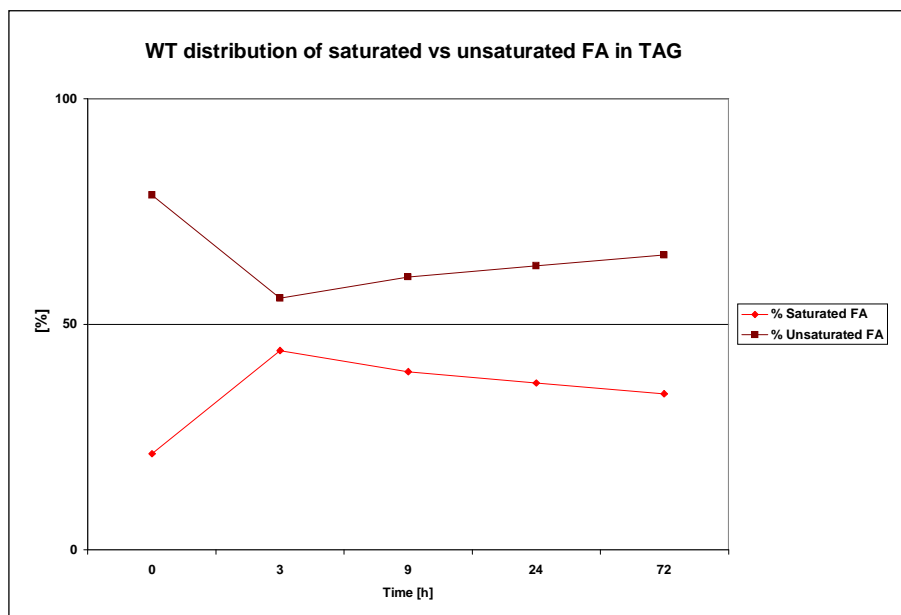


Figure 5.33: Distribution of saturated versus unsaturated FA in TAG over time, WT.

The *swe1* strain shows a lower level of TAGs in the first 3h, however this changes. At 9h, 24h and 72h the *swe1* mutants TAG levels are higher than those in WT. An increase in TAG can even be seen between 3 and 9h, which suggest again that TAG synthesis is well on the way. When comparing the TAG levels at 0 and 72h, a great difference can be seen. It suggests that TAG levels

in the *swe1* strain decrease significantly when the cells are in the stationary phase. The same observation as in WT was made concerning the amount of saturated FA in the total TAG amount. In this strain it decreases from about 31% to 17% (data not shown). However it seems that the *swe1* strain has a higher TAG consumption during the stationary phase (72h and 0h time points). Referring back to the hypothesis that Swe1p could be a TAG synthesising acyltransferase: the decreased levels of TAG at 0h might be explained by the fact that Swe1p is indeed an acyltransferase and that the balance between TAG synthesis and TAG degradation in the *swe1* mutant is disrupted. On the other hand experiments with deletion strains lacking all TAG synthesising enzymes (*dgallrolare1are2* strain) do not show residual TAG levels that could be linked to Swe1p and its acyltransferase activity (Petschnigg et al., 2009).

The *tgl3tgl4* strain shows a significantly lowered TAG level at 9h, which can mainly be explained by the dilution effect. Cells are actively dividing and in absence of lipases, the remaining TAG stock is shared between mother and daughter cells. After 9h TAG levels increase until 72h, ending up at only a slightly higher level than seen at 0h. It seems that the “*de novo*” synthesis at this point outweighs the dilution effect, replenishing the cellular TAG stores.

The *tgl3tgl4swe1* mutant does not show such a dramatic decrease at 9h, and ends up at nearly the same levels as seen at 0h. The dilution effect also comes into play, since the cells are dividing quickly. The question remains why the additional deletion of *SWE1* results in these higher levels? As stated earlier, a possible explanation could be that Swe1p has a more direct link to lipid metabolism than previously suggested. If Swe1p is directly linked to lipolysis (deletion of *SWE1* recovers the delay), then it is not far fetched to suppose it also regulates TAG synthesis. As Swe1p is a regulatory kinase, it could be involved in both synthesis and degradation of TAG. This would explain why in its absence TAG levels are higher and do not fluctuate as severely. This theory, however plausible, is in contrast with Swe1p being a DAG-acyltransferase.

While observing the distribution of saturated versus unsaturated FA in these 2 strains an interesting observation was made (**Figure 5.34**). The decrease in saturated FA content (between 72h and 7 days) seen in WT and the *swe1* mutant is also seen in the *tgl3tgl4* and *tgl3tgl4swe1* strains with a drop from 42% to 34% in both cases. This suggests that even in absence of the main lipases, TAGs

are still degraded and FAs used for β -oxidation. Tgl5p could be responsible for this degradation. When comparing **Figure 5.33** and **5.34** it is interesting to see that WT and the *swe1* mutant start off at 0h with a much higher level of unsaturated FA, and the level drops over time. It can therefore be postulated that these strains primarily cleave off unsaturated FA during TAG mobilization. The *tgl3tgl4* and *tgl3tgl4swe1* mutants on the other hand do not show such a dramatic shift in their distribution of FA during that mobilization phase. As seen in the previous sections, there is TAG degradation during the mobilization phase in the strains lacking lipases suggesting the presence of an additional lipase that counteracts the Tgl3p and Tgl4p deficiency. However while observing **Figure 5.34** it can be postulated that this additional lipase does not show such a pronounced preference for unsaturated FA. If Tgl5p is responsible for this degradation these observations suggest that it might shift its substrate preference when the cells are in different phases of growth. It cleaves off saturated FAs during the stationary phase for β -oxidation, however during the mobilization phase, it does not show such a preference.

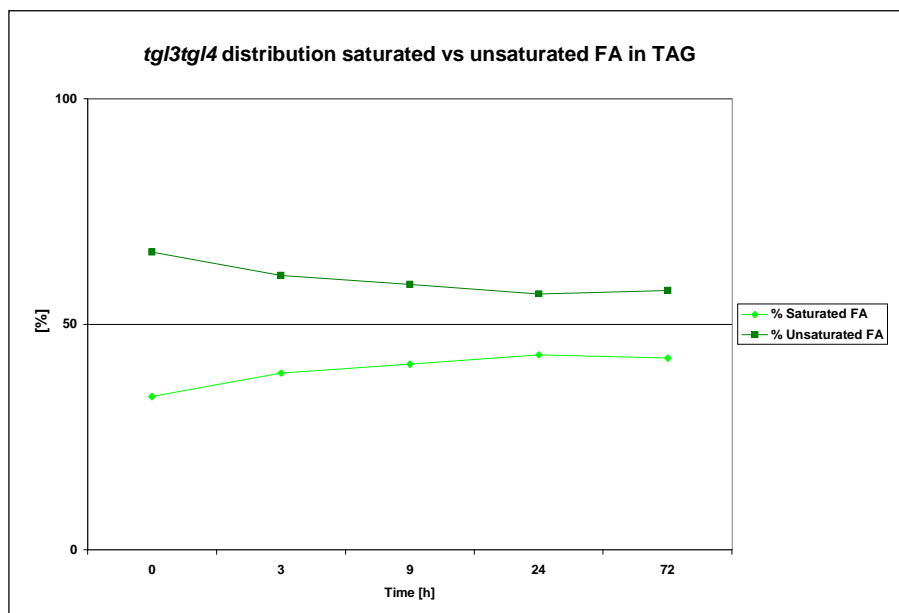


Figure 5.34: Distribution of saturated versus unsaturated FA in TAG over time, *tgl3tgl4*.

5.5.2. Diacylglycerol (DAG)

Figure 5.35 shows the development of DAG during the growth phases in all 4 strains. DAG levels seem to spike at 3h and 9h in all 4 strains, suggesting an important role of DAG during the exponential phase of yeast growth.

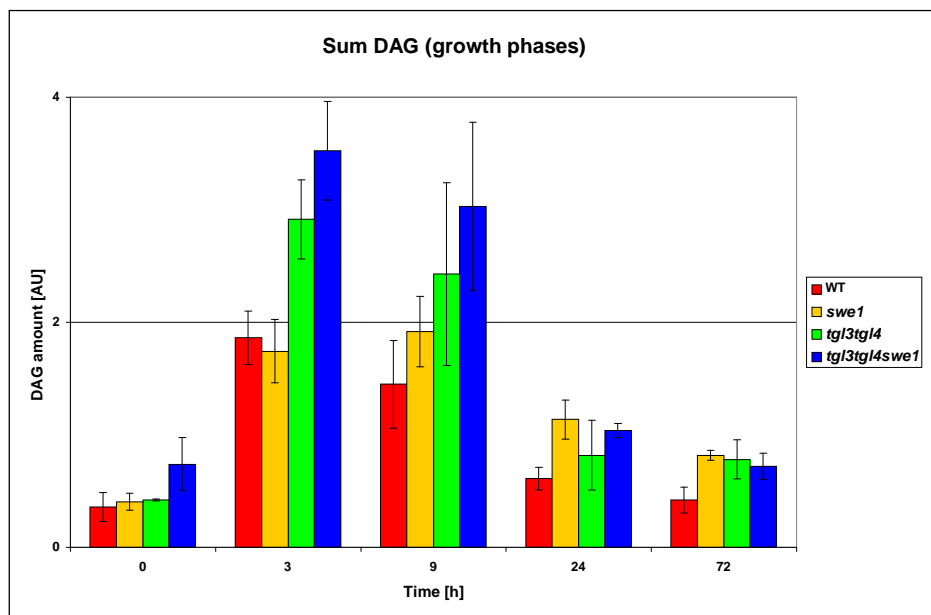


Figure 5.35: Sum DAG in all deletion strains over 72 h after inoculation into fresh media.

WT DAG levels peak at 3h and eventually return to starting levels at 72h. This might signify that DAG is not an important molecule during the stationary phase. The same trend is observed for the *tgl3tgl4* and *tgl3tgl4swe1* strains, although levels differ. As in these strains the main lipases are missing, the elevated DAG levels might be due to a different source. In the lipase deletion strains “*de novo*” synthesis might be upregulated to compensate for the need of precursors for PL membrane synthesis. However distinct lipolytic activity is observed during the first 3h after inoculation into fresh media, so maybe DAG levels are also due to TAG degradation. As observed previously, DAG levels in the *swe1* strain behave in a similar way as TAGs. As of 9h, DAG levels in the *swe1* mutant are higher than those observed in WT. They also do not reach initial levels at 72h. Referring back to the idea that Swe1p might be a DAG acyltransferase, the absence of Swe1p could explain the slightly higher levels of DAG.

5.5.3. Phosphatidic acid (PA)

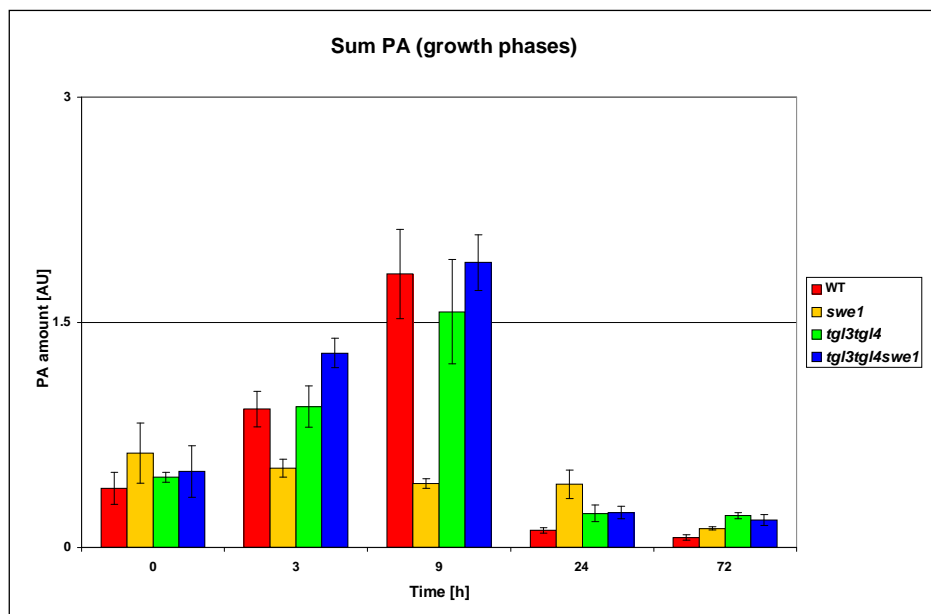


Figure 5.36: Sum PA in all deletion strains over 72 h after inoculation into fresh media.

Figure 5.36 shows the behaviour of PA in all strains during the different growth phases. WT shows an increase of PA during the lag- and log-phases of growth suggesting that PA is important for these phases. This is logical since PA is a direct precursor for membrane phospholipids. When returning to the stationary phase, WT PA levels decrease drastically. This is also in accordance with the fact that PA is a precursor, as during the stationary phase, there is not so much need for new PL. PA levels in the *swe1* mutant show a very different behaviour. They do not increase during the exponential phase and show higher levels than in the other strains upon entry into the stationary phase (~24h). This behaviour illustrates that Swe1p definitely has an effect on lipid metabolism. However the direct link is still not clear. If supposedly Swe1p has a lyso-PA acyltransferase activity, then the absence of this protein might explain the deviant behaviour of PA in this strain. This theory however is contradicted when observing the behaviour of the *tgl3tgl4swe1* strain, and its PA content. The *tgl3tgl4* and *tgl3tgl4swe1* strains show similar behaviour to WT, although their levels are slightly higher than WT when entering the stationary phase. The PA levels in WT and the lipase deficient strains suggest that PA might not directly originate from lipolysis. Either PA is produced mainly by “*de novo*” synthesis, or the lipase

deficient strains have an additional compensatory mechanism that normalizes PA levels in absence of lipolysis. If supposedly Swe1p is a lyso-PA acyltransferase, the additional deletion of *SWE1* should also decrease the PA levels in the *tgl3tgl4swe1* strains. However, if the absence of lipases kick-starts “*de novo*” synthesis in lipase deficient strains, then this effect would be counteracted.

5.5.4. Phosphatidylinositol (PI)

Figure 5.37 shows PI levels in all 4 strains during the different phases of growth. All strains show similar behaviour in their PI content. It rises in the first 3h, and then drops at 9h. This could be correlated to cell size. At 9h the cells are dividing quickly and their size is on average smaller as the population is unsynchronised. PI is also an important molecule in signalling pathways, and this drop could signify that during the exponential phase of growth PI is very actively required for biochemical processes. Upon entry into quiescence PI levels in WT, the *tgl3tgl4* and *tgl3tgl4swe1* mutants seem to stay relatively constant, which is also explained by the fact that PI is a component of membranes and that stationary cells do not grow anymore. It could also mean that the signalling pathways where PI is involved occur mainly during the lag- and the log-phase of growth.

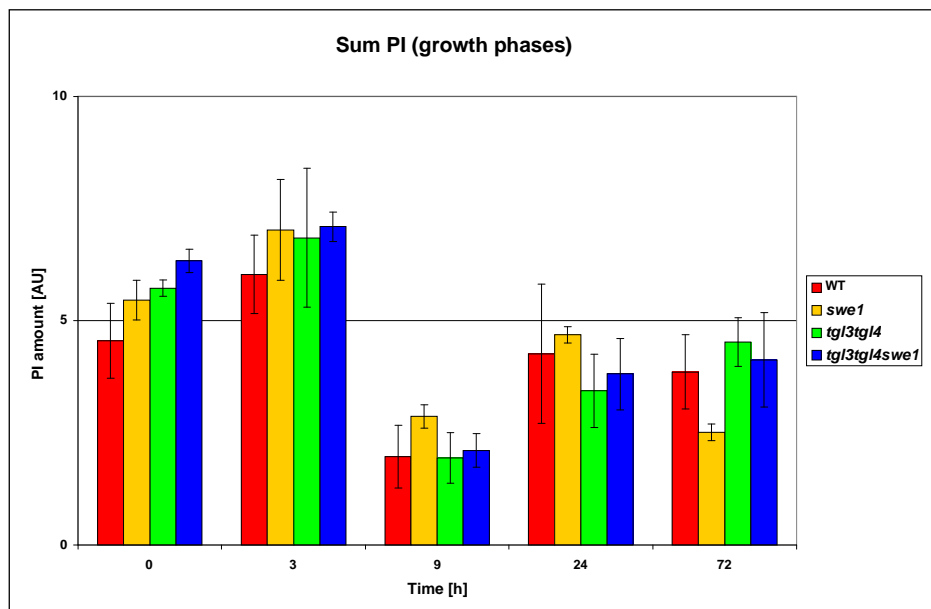


Figure 5.37: Sum PI in all deletion strains over 72 h after inoculation into fresh media.

PI levels in the *swe1* mutant are lower at 72h than those of the other strains. PI and Swe1p are linked to the sphingolipid (SL) metabolism. The SGD states that Swe1p phosphorylates Orm1p and Orm2p, major regulators of the SL metabolism. As Swe1p is a morphogenesis check-point, it is not implausible to think that its activity is mainly inhibitory. N. Chauhan also suggested the idea of Swe1p being a lipid sensor. If Swe1p has a more direct link to lipid metabolism and its regulation, it is logical to think that part of its activity needs to be sensory. If Swe1p negatively regulates PI use for SL production, then the absence of this protein explains the lower levels of PI, as they are used for SL production. On the other hand this would be reflected throughout the measured time points. When observing the 9h time point, PI levels in the *swe1* strain are slightly higher. When comparing the PI levels of all strains at 72h and 0h, all strains show higher PI levels at 0h. This means that during their stationary phase between 3 and 7 days, their PI content changes. An explanation for this might be that stationary cells need a different PL content with different physical properties.

5.5.5. Phosphatidylserine (PS)

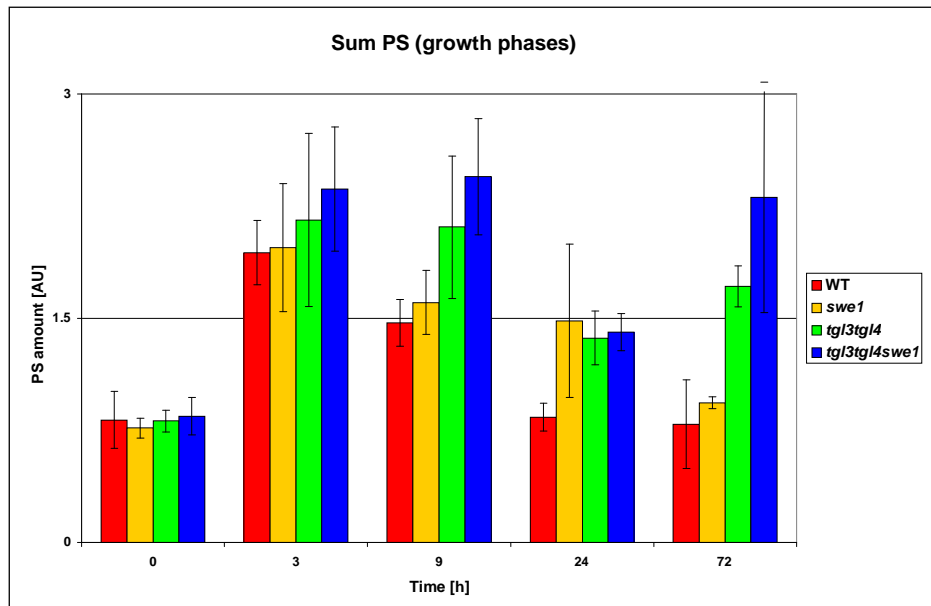


Figure 5.38: Sum PS in all deletion strains over 72 h after inoculation into fresh media.

Figure 5.38 shows the development of PS during growth in all 4 deletion strains. At 0h all 4 strains start of at the same level. This suggests that PS levels stay the same during the lag-phase of

growth. While comparing the 72h and 0h time points, a great difference can be seen in PS levels. While WT and the *swe1* mutant display similar levels, the *tgl3tgl4* and the *tgl3tgl4swe1* strains show a big difference. This suggests that the lipases or absence thereof, affect PS levels during the stationary phase. Moreover it seems that during stationary phase PS levels in those mutants are very dynamic. The excess PS observed at 72h seems to be either degraded or funnelled into PE or PC production during the stationary phase. The absence of lipases shows the most pronounced effect on PS levels upon entry into quiescence. This is a further clue to the theory mentioned earlier. If the lipase mutants have a compensatory mechanism that kick-starts “*de novo*” synthesis, then this would also reflect on PS levels. However this would be reflected more in the lag- and log phases of growth. Maybe that compensatory mechanism stays active throughout the cell’s division and growth to compensate for the absence of TAG degradation. Another possible explanation for the unusual PS levels could be the fact that Cho1p is a membrane bound enzyme. It is then not unusual to think that PL composition around this enzyme has an effect on its activity. If the lack of lipases affects the PL composition, this could increase (or decrease) its activity. A possible experiment to confirm this theory would be to test the activity of Cho1p in vitro, using different PL compositions to create embedding micelles (Carman and Zeimet, 1996).

Another interesting explanation to these elevated PS levels would be the involvement of the acyl-CoA binding protein Acb1p. Acb1p is a protein involved in transporting newly synthesised FAs from the fatty acid synthase complex to locations where they are needed (Shjerlin et al., 1996). Feddersen et al. (2007) suggested an additional function for Acb1p. They postulate that the Acb1p-Acyl-CoA complex regulates the transcription of certain PL synthesising enzymes. In absence of Acb1p, the complex is not formed and those genes are up-regulated. One of those genes encodes Cho1p, the PS synthesising enzyme (Carman and Zeimet, 1996). Although their work analyzed the effect of the absence of Acb1p on those genes, one could speculate that the absence of certain FAs, that bind Acb1p, might have the same effect, as no Acb1-Acyl-CoA complex is formed and thus the genes are up-regulated. Theoretically, lipase mutants should be deficient in FAs, especially in the lag-phase. This might in turn promote the expression of *CHO1*, and elevate PS levels at later stages of growth. However our observations do not support this theory entirely, as there is a pronounced degradation of TAGs during the lag-phase. Nevertheless it was also observed

that this degradation does not show a preference for certain TAG species. This might suggest that only certain FAs are involved in the transcriptional regulation of PL synthetic genes.

5.5.6. Phosphatidylethanolamine (PE)

Figure 5.39 shows the development of PE during growth. WT and the *swe1* mutant show similar behaviour: PE increases over the first 9h, then decreases upon entry into quiescence. Their levels however increase again after 72h to reach the 0h (7day) time point. This graph suggests that Swe1p does not have an effect on PE levels. PE levels in the *tgl3tgl4* and *tgl3tgl4swe1* strains peak at 3h, followed by a drop, and at 72h they rise again. Their levels decrease during the stationary phase, to reach the 7day levels. These changes observed after 72h could be due to a change in membrane PL composition, with stationary cells having different requirements for their membranes. However how the different deletions play a role is still unclear. Elevated PE levels in these 2 strains, however, is a logical consequence of the elevated PS levels observed earlier as PS is a direct precursor to PE. Another reason for elevated PE levels could be found in the theory described by Feddersen et al. (2007) which also includes the PE synthesising enzymes. The higher levels of PE could, as a consequence, also be due to higher expression of *PSD* genes.

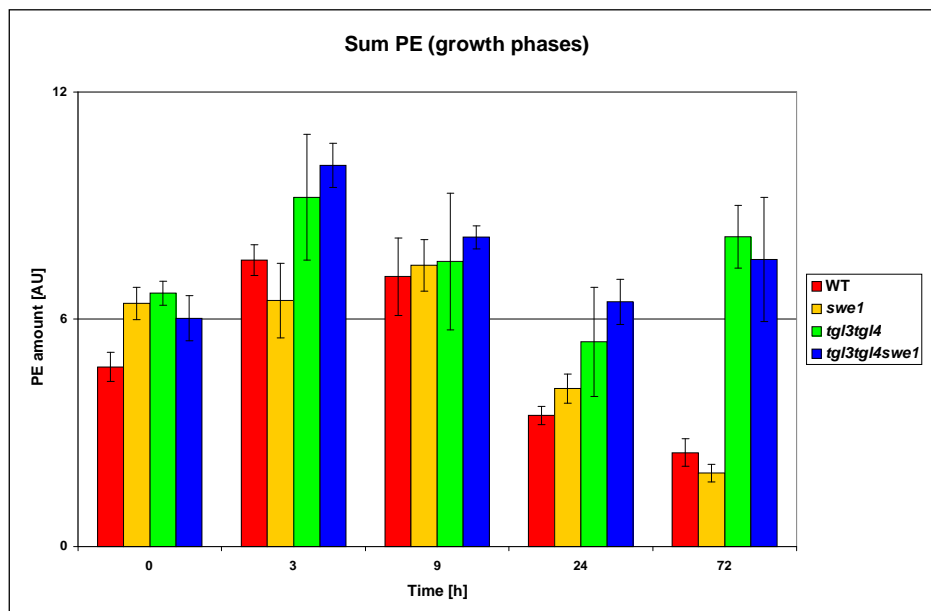


Figure 5.39: Sum PE in all deletion strains over 72 after inoculation into fresh media.

The higher DAG levels observed during the log phase of growth in these strains might also be an explanation for the high PE levels. DAG can be a direct and indirect precursor for PE synthesis, as there are two pathways that produce PE. Higher DAG levels might push the cells to produce more PE by the Kennedy pathway to prevent DAG toxicity.

5.5.7. Phosphatidylcholine (PC)

Figure 5.40 shows PC levels over time in all 4 strains. All four strains show similar tendencies: the PC levels peak at 3h. Cells then start the exponential phase of growth and require a lot of PC to create membranes. However when observing the changes between 72h and 7 days, the behaviour is similar than seen in PS and PE. All 4 strains show PC levels that rise during stationary phase. The same explanation as stated in the previous section may apply, that membrane PL composition during the stationary phase of growth varies, even though cells do not grow per se. The elevated PC levels at 72h in the lipase mutant strains might again be explained by the theory suggested by Feddersen et al. (2007). The PC synthesising enzymes are also transcribed at a higher level when *Acb1p* is absent, so one might suppose that this is also the case when FAs are scarce. This theory might explain the higher levels of PL observed in general, however it is in contradiction with the postulate that lipase mutants counteract lipolysis deficiency by activating “*de novo*” synthesis”. If this was the case then FA’s would be present and the PL synthetic genes would not be transcribed at a higher level. On the other hand if the “*de novo*” synthesis is active, then the higher levels of PLs in these strains could be explained also by increased incorporation of FAs into PL. It has to be mentioned, however, that even if certain genes are transcribed at a higher level, this does not necessarily allow conclusions on the activity of the encoded enzymes.

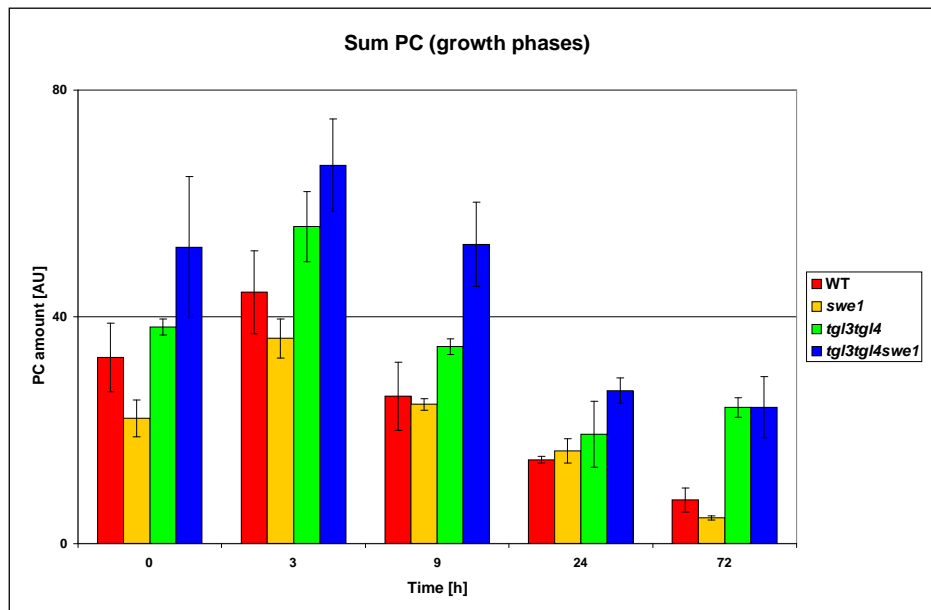


Figure 5.40: Sum PC in all deletion strains over 72 h after inoculation into fresh media.

5.6. Further discussion

Referring back to the theory formulated by Feddersen et al. (2007) stating an up regulation of PL synthesising enzymes in absence of Acb1p (and maybe also of FAs) and the alternative theory that lipase mutants have a compensatory mechanism to counteract the absence of lipolysis, a third point of view emerges where these two theories can be linked. If one supposes that Acb1 is a FA sensor and in absence of lipolysis, FA levels are low, a possible hypothesis could be that Acb1p senses low FA levels originating from lipolysis and activates an alternative way of synthesising PLs for growth. It might kick-start “*de novo*” synthesis and up-regulate transcription of PL synthesising enzymes to allow normal growth. This would result in a by-pass mechanism to compensate for lack of TAG degradation. This theory is more likely as Acb1 is also reported to interact with the fatty acid synthase complex, involved in “*de novo*” synthesis, to transport newly synthesised acyl-CoAs to acyl-CoA utilising processes (Shjerlin et al., 1996).

Another interesting player that might be involved in this theory is Crd1p. Crd1p is a protein in the inner membrane of mitochondria involved in the production of cardiolipin. A quick search on the STRING database for predicted protein interactions yielded the following picture on Crd1p, which can be seen in **Figure 5.40**. This protein is interesting as it links Swe1p, Acb1p and PL

biosynthesis. Crd1p is predicted to interact with a few PL synthetic enzymes, although the type of interaction is not clear. It is also predicted to interact with Swe1p and with Acb1p. These predicted interactions alone underline how important lipid metabolism and homeostasis is for cell cycle progression and regulation.

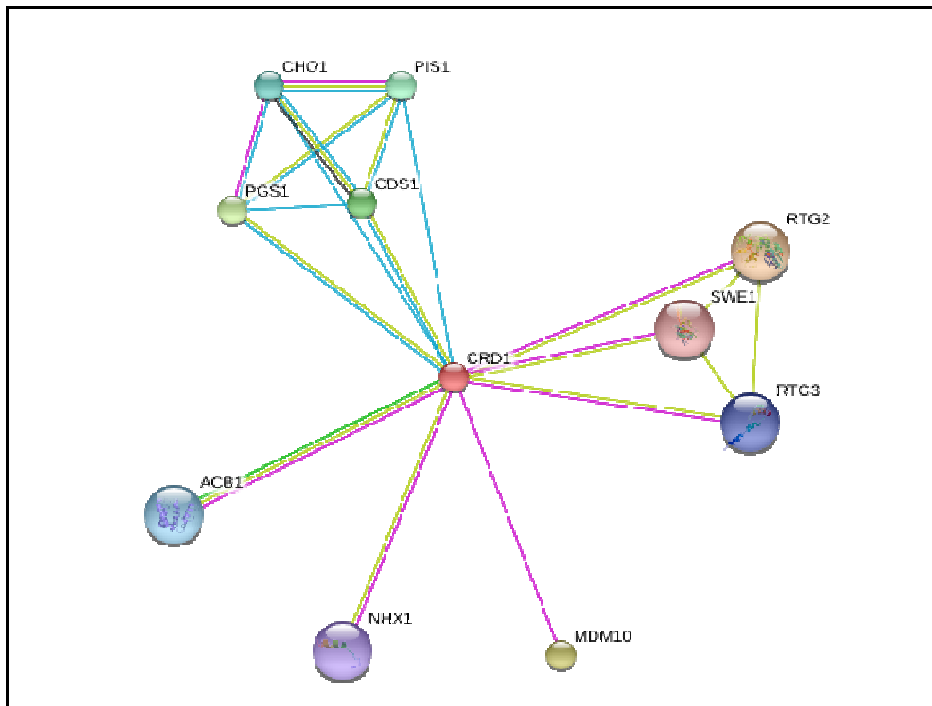


Figure 5.41: Predicted interactions of Crd1p according to the STRING database.

A possible model for these interactions can be seen in **Figure 5.41**. The nature of the interactions between Crd1p and different metabolic pathways is not yet known, but it emerges that Crd1p might play a central role in coordinating lipid metabolism and its link to cell cycle.

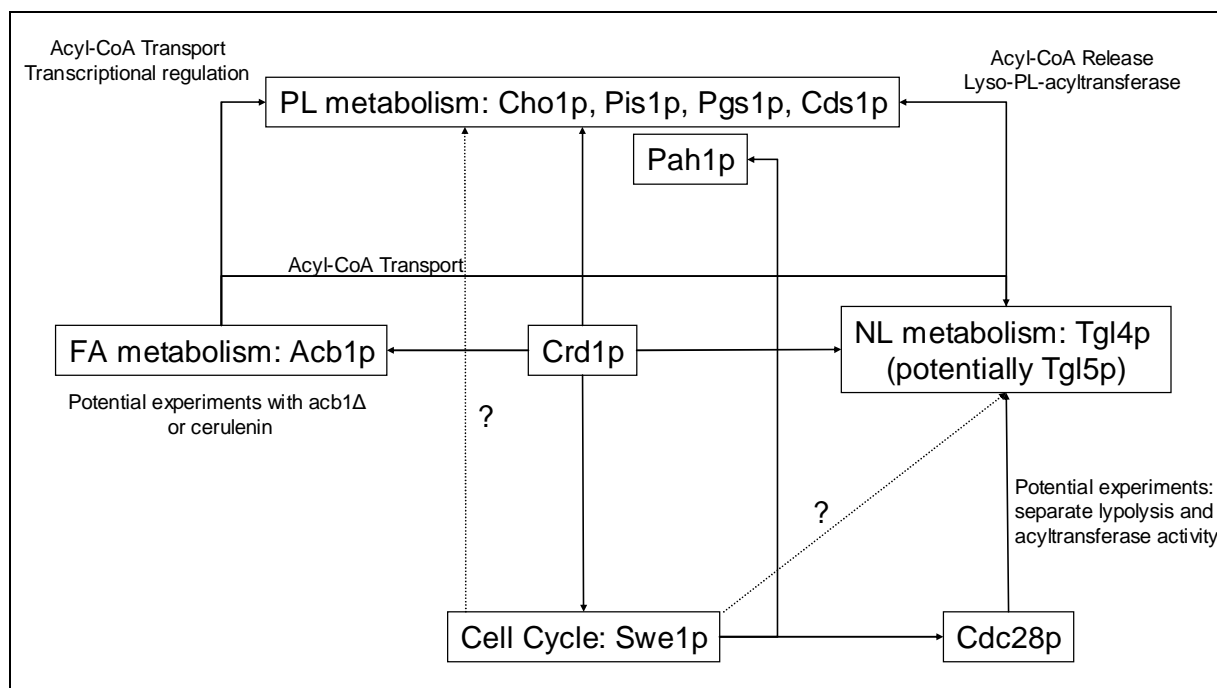


Figure 5.42: Model involving Crd1p in lipid metabolism and cell cycle regulation.

6. Conclusions

Observations made in the lipid profile of the 4 strains in question gave interesting insights into the effect of *SWE1* deletion on lipid metabolism. However looking at the lipid profiles alone did not elucidate those interactions entirely. Many unanswered questions remain, that would need to be answered by further experiments. Interesting points for further work would be to find out what causes the TAG degradation in the *tgl3tgl4* and *tgl3tgl4swe1* strains in the first 60min after initiation of the cell cycle? What causes the drop in PC in those strains during the same time period? An interesting target to answer these questions would be the lipase Tgl5p.

One aim of these experiments was to see if the delay in cell cycle observed by FACS analysis in the *tgl3tgl4* strain and the recovery of this delay by additional deletion of *SWE1* could also be seen in the lipid profiles. This might have given insight into which classes or species of lipids were responsible for this delay. The previously described delay (and its recovery) was, however, not distinctively observed in the lipid profiles, although there were a few observations that need to be mentioned. The lipid profiles of the *tgl3tgl4* and *tgl3tgl4swe1* strains show very similar behaviour,

the main conclusion being that the additional deletion of *SWE1* in the *tgl3tgl4* mutant seems to emphasize the levels and behaviour of most lipid classes over time. An interesting point of further study might be to elucidate if Tgl5p also acts as a target protein of Cdc28p. The profiles of WT and the *swe1* mutant are also quite similar in general; the main disparity being that the *swe1* mutant shows dissimilarity in certain PA and PI species. This could be due to the involvement of Swe1p in the sphingolipid metabolism, for which PI, and indirectly PA, are precursors. It would be interesting to check the sphingolipid levels in these strains, to see if a flow of lipid species into this pathway can be determined.

Swe1p clearly appears to have an impact on lipid composition, although a model for its specific activity could not yet be determined. The generally decreased lipid levels in the *swe1* strain can partially be explained by the hypothesis that Swe1p acts as a DAG-acyltransferase. However this theory needs to be confirmed as it is solely based on the observation that Swe1p contains a motif suggesting acyltransferase activity. The generally elevated lipid levels in the *tgl3tgl4swe1* strain are harder to explain, as they contradict the theory of DAG-acyltransferase activity. It would be interesting to do *in vitro* experiments to determine whether Swe1p presents this feature, and if it does, which kind of acyltransferase it would be as certain observations also suggest a lyso-PA acyltransferase activity.

Lipid profiling is a valuable tool to analyse the lipid composition and changes thereof in yeast. However this MS based technique should always be complemented by other experimental techniques to confirm the observations that were made. Unfortunately this was beyond the time-scope of this thesis.

These experiments have given certain insights into how Swe1p might affect lipid composition during the cell cycle, and they have suggested a more direct link of Swe1p to lipid metabolism than the one described by its interaction with Cdc28p. The specific role of Swe1p in lipid metabolism remains unclear at this point. Nevertheless some interesting discoveries were made when analysing the potential interaction partners of Swe1p. Acb1p and Crd1p offer themselves as a very interesting subject of study in the future to determine whether these three proteins might act

in concert as lipid sensors during the cell cycle, and thus directly regulating its progression or delay.

7. Materials & Methods

7.1. Strains and Media

The used strains can be seen in **Table 7.1**. Their genotype was confirmed by PCR (not depicted here) and the primers used can be seen in **Table 7.2**.

Table 7.1: List of strains

Strains	Genotype	Source
BY4741	<i>MAT a; his3Δ 1; leu2Δ 0; met15Δ 0; ura3Δ 0</i>	Euroscarf
<i>Tgl3ΔTgl4Δ</i>	<i>MAT a; his3Δ1; leu2Δ0; lys2Δ0; ura3Δ0; YMR313c::kanMX4; YKR089c::kanMX4;</i>	Kurat et al. (2006)
<i>Swe1Δ</i>	<i>MAT a; his3□1; leu2□0; met15□0; ura3□0; YJL187c::kanMX4</i>	Euroscarf
<i>Tgl3ΔTgl4ΔSwe1Δ</i>	<i>MAT a; his3Δ1; leu2Δ0; lys2Δ0; ura3Δ0; YMR313c::kanMX4; YKR089c::kanMX4; YJL187c::kantMX4</i>	N. Chauhan

Table 7.2: Primers

Primer	
Tgl3 Forward	CCTAGGTCTGAAAATTCAACCCTAACCC
Tgl4 Forward	CTTAAGGGGTTTAAAAAAAGTAGGGTAAACTAG
Swe1 Forward	GTGTGTTAACTATCCTGCACATCATCTTG
Kanmx4 Reverse	GAAACAACCTCTGGCGCATCG

Two types of Media were used during these experiments. Their composition can be seen in **Table 7.3**.

Table 7.3: Media composition

YPD Media in H ₂ O bidest.		
Components	Company	Amount
Yeast Extract	BD	10 g/l
Peptone	BD	20 g/l
Glucose Monohydrate	Roth	22 g/l
YNB Media in H ₂ O bidest.		
YNB-(NH ₄) ₂ SO ₄ -AA	Difco	1.7 g/l
(NH ₄) ₂ SO ₄	Merck	5 g/l
Amino Acid Stock 50x		20 ml/l
Glucose Monohydrate	Roth	22 g/l

7.2. Synchronisation

The method for synchronisation chosen for this work was density gradient centrifugation, which separates quiescent from non quiescent/dead cells. (Modified after Allen et al., 2006, for detailed SOP c.f Annexe)

7.3. Growth

An ONC and a 7DC of the selected strain were made in YPD media, 30°C, and 180 rpm. After synchronisation the cells were inoculated in fresh YNB media. 5×10^8 cells were inoculated in a 250 ml flask with 50 ml YNB media. They were grown at 30°C and 180 rpm. Every 30 minutes the cells were counted, harvested, pelleted and frozen in preparation for LE.

7.4. Lipid extraction and UPLC-qTOF-MS measurements

The lipids were extracted according to the Standard Operating Procedure of our lab (Modified after Folch et al., 1957). The isolated lipids were then separated by UPLC, ionised by ESI and detected by qTOF-MS. (For detailed SOP of LE, please refer to Annexe). The internal standard mix (IST) used during the LE procedure is described in **Table 7.3**. For each sample 50 µl of IST Mix was used.

Table 7.4: IST Mix composition (C/M: Chloroform/Methanol)

Lipid	Concentration [mg/ml] in C/M 2:1
DAG 28:0 (Avanti)	0.05
TAG 36:0 (Larodan)	0.05
TAG 45:0 (Larodan)	0.05
TAG 51:0 (Larodan)	0.05
TAG 57:0 (Larodan)	0.05
PC 24:0 (Avanti)	0.05
PC 34:0 (Avanti)	0.05
PC 38:0 (Avanti)	0.05
PE 24:0 (Avanti)	0.05
PE 34:0 (Avanti)	0.05
PS 34:0 (Avanti)	0.05
PA 24:0 (Avanti)	0.05
PA 28:0 (Avanti)	0.05
PA 34:0 (Avanti)	0.05

The chromatographic separation was performed using a Waters Acquity UPLC[®]. The analysis was performed on a Acquity UPLC[®] BEH C18 hydrophobic column (1.7µm, 2.1*150mm), over a time period of 50min, using a mobile phase (MP) gradient with a flow of 180µl/min.

The mobile phase composition was as following:

- Mobile Phase 1 (MP1) : Methanol (J.T. Baker)/H₂O (Roth) 1:1 ; 0.1% HCOOH (Roth), 1% NH₄Ac (Merck)
- Mobile Phase 2 (MP2) : Isopropanol (Roth); 0.1% HCOOH, 1% NH₄Ac

The gradient was as following:

- Initial ratio : 55 % MP1 and 45 % MP2
- 30min: 10 % MP1 and 90 % MP2
- 32min: 0 % MP1 and 100 % MP2
- 43min: 55 % MP1 and 45 % MP2

The mass spectrometric analysis (positive and negative ionisation) was performed using a Waters Synapt[®] Q-TOF HDMS. The positive electro-spray ionisation was performed with a scan time of 1.5 s over a mass/charge range from 50 to 1800. The reference mass of the LeuEnk peptide standard was 556.2771 g/mol. The capillary voltage was set at 2.4kV, the sampling cone at 45V and the extraction cone at 4.0V. In the negative ionisation mode the capillary voltage was set at 2kV, the sampling cone at 50V and the extraction cone at 4.5V. The gradient remained the same for both types of analysis.

7.5. FACS analysis (fluorescence activated cell sorting)

Cell cycle analysis was performed by fluorescence activated cell sorting (FACS) analysis. Aliquots of stationary phase cells grown in YPD media were withdrawn and cells were spun down, washed in distilled water, fixed in 70% ethanol, and treated with 10 mg/ml RNaseA in 50mM Tris-HCl (pH 7.5) for 4h at 37°C. After resuspension in 50mM Tris-HCl (pH 7.5), Proteinase K (2mg/ml) was added and cells were further incubated for 1h at 50°C. DNA was stained with 1mM SYTOX Green (Invitrogen, Inc.) in 1x PBS (pH 8), sonicated at low intensity, and scanned in BD FACS Aria flow cytometry system from BD, using BD FACSDiva software (For a step by step SOP, please refer to the Annexe section).

8. Annexe

8.1. SOP

8.1.1. RediGrad Centrifugation

- Prepare centrifugation tubes: wash with EtOH and dry in the drying cupboard
- Divide 50ml 7DC into 4 equal volumes and transfer to 15ml falcons (Greiner Bio One)
- Centrifugation: Eppendorf Tabletop Centrifuge, 3500rpm, 5min
- Remove supernatant (media)
- Add 2ml Tris Buffer (pH 7,5) and resuspend pellet
- Centrifugation: 3500rpm, 5min
- In parallel:
 - Prepare centrifugation tubes: add 9ml RediGrad (GE Healthcare) solution and 1ml NaCl 1,5M
 - Creation of a gradient: centrifugation, Beckmans high-speed centrifuge, 19000rpm, 15min
- When cells are done: add 2ml Tris buffer pH 7,5 and resuspend pellet
- Centrifugation: 3500rpm, 5min
- Add 1ml Tris buffer pH 7,5 and resuspend pellet
- Remove the centrifugation tubes GENTLY from the high-speed centrifuge and place in a rack. (do not disrupt gradient)
- Pipette the cell suspension GENTLY down the side of the tubes onto the gradient solution in the centrifugation tube (cells should stay on the surface)
- Place the tubes GENTLY in the table-top centrifuge: 400g (1495rpm), 60min
- Gently pipette lower band into 15ml Falcon tubes (4-5ml). (Upper band: non-quiescent/dead cells)
- Add 10ml Tris buffer pH 7.5, and shake thoroughly! (disrupts the gradient)
- Centrifugation: Eppendorf tabletop centrifuge, 3500rpm, 5min
- Remove supernatant, add 2ml Tris buffer and resuspend
- Centrifugation: Eppendorf tabletop centrifuge, 3500rpm, 5min

-
- Repeat washing steps twice
 - Resuspend in Tris buffer (Volume as required)

8.1.2. FACS

- Add appropriate amount of cells to 500µl of 100% EtOH (Roth) (storage at 4°C for several months)
- Pellet cells at maximum speed for 10min at 4°C (Eppendorf Centrifuge 5415R)
- Remove supernatant (EtOH) and add 500µl of ddH₂O, vortex
- Pellet cells at maximum speed for 10min at 4°C
- Remove ddH₂O, and add 200µl 50mM Tris Buffer pH 7,5 and 4µl RNAase (Roche) 20mg/ml
- Vortex and incubate at 37°C, 550rpm for 4h
- Pellet cells at maximum speed for 10min at 4°C
- Remove supernatant
- Add 80µl 50mM Tris Buffer pH 7,5 and 20µl Proteinase K (Roche) 5mg/ml
- Vortex and incubate at 50°C, 550rpm for 1h (Eppendorf Thermomixer compact)
- Pellet cells at maximum speed for 5-10min at 4°C. Remove supernatant, and add 500µl PBS 1x (can be left overnight, not more)
- Sonicate for 1,5min
- Vortex and transfer to FACS tubes (!!Label Tubes before transfer!!)
- Add 1µl 1mM SYTOX Green stain (Invitrogen Inc.), vortex
- Leave at RT for a few minutes before measurements

8.1.3. LE

- Grow cells to desired growth phase
- Harvest cells ($5 \cdot 10^8$ cells) 3500rpm, RT.
- Remove supernatant quantitatively
- Freeze pellet in liquid N₂ and store at -80°C
- Add 5ml chloroform (Sigma-Aldrich)/methanol (Roth) 2:1 to pellet and transfer to screw cap 25ml Pyrex tube
- Add 50µl IST Mix to each sample

-
- Add 1ml methanol washed glass beads
 - Shake on Heidolph Multi Reax for 30min, level 10 at 4°C
 - Add 1ml 0.034% MgCl₂
 - Shake on evapor mixer for 10min, level 10 at 4°C
 - Centrifuge 3000rpm, 5min, RT
 - Discard aqueous upper phase (not interphase)
 - Add 2ml artificial upper phase MeOH/H₂O/CHCl₃ (48:47:3)
 - Centrifuge 3000rpm, 5min, RT
 - Discard aqueous upper phase (not interphase)
 - Transfer organic lower phase to a 15ml Pyrex tube
 - With blue tips directly out of glass beads
 - Proteins remain on glass beads
 - Get rid of glass beads later
 - Evaporate organic solvents in N₂ stream
 - Dissolve lipids in 1 mlC/M 2:1
 - Transfer to autosampler vials without glass beads
 - Dilute 1:20 before positive ionisation UPLC-MS analysis, use undiluted sample for negative ionisation UPLC-MS analysis

9. References

- Allen C., Büttner S., Aragon A. D., Thomas, J. A., Meirelles O., Jaetao J. E., Benn D., Ruby S. W., Veenhuis M., Madeeo F., Werner-Washburne M. (2006) Isolation of quiescent and nonquiescent cells from yeast stationary-phase cultures. *JCB* **174**(1): 89-100.
- Asano S., Park J. E., Sakchaisri K., Yu L. R., Song S., Supavilai P., Veenstra T. D., Lee K. S. (2005) Concerted mechanism of Swe1/Wee1 regulation by multiple kinases in budding yeast. *EMBO J* **24**(12): 2194-2204.
- Bielewska A., Perry D. K., Hannun Y. A. (2001) Determination of Ceramides and Diglycerides by the Diglyceride Kinase Assay. *Anal Biochem* **298**: 141-150.
- Carman G. M., Zeimet G. M. (1996) Regulation of Phospholipid Biosynthesis in the Yeast *Saccharomyces cerevisiae*. *J Biol Chem* **271**(23): 13293-13296.
- Dowhan W. (1997) Molecular Basis for Membrane Lipid Diversity: Why are there so many lipids? *Annu Rev Biochem* **66**: 199-232.
- Feddersen S., Neergaard T.B.F., Knudsen J., Faergeman N. (2007) Transcriptional regulation of phospholipid biosynthesis is linked to fatty acid metabolism by an acyl-CoA-binding-protein-dependent mechanism in *Saccharomyces cerevisiae*. *Biochem J* **407**: 219-230.
- Gray J. V., Petsko G. A., Johnston G. C., Ringe D., Singer R. A., Werner-Washburne M. (2004) “Sleeping Beauty”: Quiescence in *Saccharomyces cerevisiae*. *Microbiol Mol Biol Rev* **68**(2): 187-206.
- Griffiths A. J. F., Gelbart W. M., Miller J. H., Lewontin R. C. (1999) Modern Genetic Analysis. W. H. Freeman and Company (New York), ISBN-10: 0-7167-3118-5.
- Harvey S. L., Charlet A., Haas W., Gygi S. P., Kellogg D. R. (2005) Cdk1-Dependent Regulation of the Mitotic Inhibitor Wee1. *Cell* **122**(3): 407-420.
- Kurat C. F., Wolinski H., Petschnigg J., Kularachchi S., Andrews B., Natter K., Kohlwein S. D. (2009) Cdk1/Cdc28-Dependent Activation of the Major Triacylglycerol Lipase Tgl4 in Yeast Links Lipolysis to Cell-Cycle Progression. *Mol Cell* **33**(January 16): 53-63.
- Kurat C.F., Natter K., Petschnigg J., Wolinski H., Scheuringer K., Scholz H., Zimmermann R., Leber R., Zechner R., Kohlwein S.D. (2006) Obese Yeast: Triglyceride Lipolysis Is Functionally Conserved from Mammals to Yeast. *J Biol Chem* **281**(1): 491-500.
- Laporte D., Lebaudy A., Sahin A., Pinson B., Ceschin J., Daignan-Fornier B., Sagot I (2011) Metabolic status rather than cell cycle signals control quiescence entry and exit. *J Cell Biol* **192**: 949-957.

-
- Lew D. (2003) The morphogenesis checkpoint: how yeast cells watch their figures. *Curr Opin Cell Biol* **15(6)**: 648-653.
 - Lodish H., Berk A., Kaiser C. A., Krieger M., Scott M. P., Bretscher A., Ploegh H., Matsudaira P. (2007) *Molecular Cell Biology*. (Sixth Edition) W. H. Freeman and Company (New York), ISBN-13: 978-0-7167-7601-7.
 - Petschnigg J., Wolinski H., Kolb D., Zellnig G., Kurat C. F., Natter K., Kohlwein S.D. (2009) Good Fat, Essential Cellular Requirements for Triacylglycerol Synthesis to Maintain Membrane Homeostasis in Yeast. *J Biol Chem* **284(45)**: 30981-30993.
 - Rajakumari S., Grillitsch K., Daum G. (2008) Synthesis and turnover of non-polar lipids in yeast. *Prog Lipid Res* **47**: 157-171.
 - Rajakumari S., Daum G. (2010) Multiple Functions as Lipase, Steryl Ester Hydrolase, Phospholipase, and Acyltransferase of Tgl4p from the Yeast *Saccharomyces cerevisiae*. *J Biol Chem* **285(21)**: 15769-15776.
 - Richardson H., D. J. Lew, M. Henze, K. Sugimoto, S. I. Reed. (1992) Cyclin-B homologs in *Saccharomyces cerevisiae* function in S phase and in G2. *Genes Dev* **6**: 2021-2034.
 - Shjerling C.K., Hummel R., Hansen J.K., Borsting C., Mikkelsen J.M., Kristiansen K., Knudsen J. (1996) Disruption of the Gene Encoding the Acyl-CoA-binding Protein (*ACB1*) Perturbs Acyl-CoA Metabolism in *Saccharomyces cerevisiae*. *J Biol Chem* **271(37)**: 22514-22521.
 - Sherman F. (2002) Getting started with yeast. *Methods Enzymol.* **350**: 3-41.
 - Singh G. P., Volpe G., Creely C. M., Groetsch H., Geli I. M., Petrov D. (2006) The lag phase and G1 phase of a single yeast cell monitored by Raman microspectroscopy. *J. Raman Spectrosc* **37**: 858-864.
 - Taus C., Diploma Thesis 2010, University of Graz.
 - Toker A. (2005) The biology and biochemistry of diacylglycerol signaling. *EMBO reports* **6**: 310-314.
 - Trotter P. J. (2001) The Genetics of Fatty Acid Metabolism in *Saccharomyces Cerevisiae*. *Annu Rev Nutr* **21**: 97-119.
 - Weberhofer B, Diploma Thesis 2010, University of Graz.
 - Werner-Washburne M., Braun E., Johnston G. C., Singer R. A. (1993) Stationary Phase in the Yeast *Saccharomyces cerevisiae*. *Microbiol Rev* **57(2)**: 383-401.

-
- Wittenberg C., K. Sugimoto, and S. I. Reed. (1990) G1-specific cyclins of *S. cerevisiae*: cell cycle periodicity, regulation by mating pheromone, and association with the p34CDC28 protein kinase. *Cell* **62**: 225-237.
 - Young B. P., Shin J. J. H., Orij R., Chao J. T., Li S. C., Guan X. L., Khong A., Jan E., Wenk M. R., Prinz W. A., Smits G. J., Loewen C. J. R. (2010) Phosphatidic Acid Is a pH Biosensor That Links Membrane Biogenesis to Metabolism. *Science* **329(5995)**: 1085-1088.
 - Zanghellini J., Natter K., Jungreuthmayer C., Kurat C. F., Gogg-Fassolter G., Kohlwein S. D., von Gruenberg H. H. (2003) Quantitative modeling of triacylglycerol homeostasis in yeast--metabolic requirement for lipolysis to promote membrane lipid synthesis and cellular growth. *FEBS J* **275(22)**: 5552-5563.